



# LUND UNIVERSITY

## A numerical model to simulate short-term beach and dune evolution

Zhang, Jie

2021

*Document Version:*

Publisher's PDF, also known as Version of record

[Link to publication](#)

*Citation for published version (APA):*

Zhang, J. (2021). *A numerical model to simulate short-term beach and dune evolution*. Water Resources Engineering, Lund University.

*Total number of authors:*

1

### General rights

Unless other specific re-use rights are stated the following general rights apply:

Copyright and moral rights for the publications made accessible in the public portal are retained by the authors and/or other copyright owners and it is a condition of accessing publications that users recognise and abide by the legal requirements associated with these rights.

- Users may download and print one copy of any publication from the public portal for the purpose of private study or research.
- You may not further distribute the material or use it for any profit-making activity or commercial gain
- You may freely distribute the URL identifying the publication in the public portal

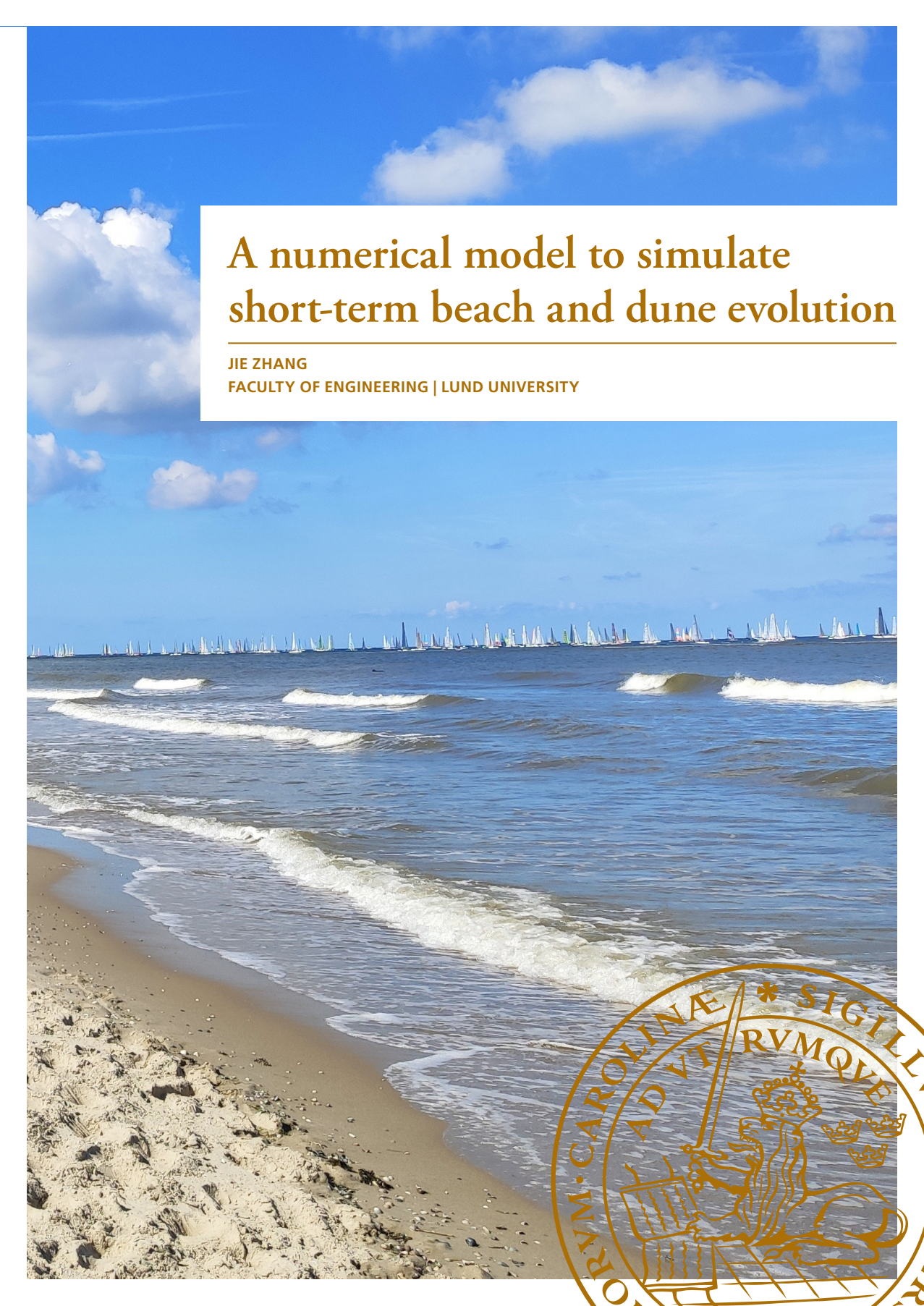
Read more about Creative commons licenses: <https://creativecommons.org/licenses/>

### Take down policy

If you believe that this document breaches copyright please contact us providing details, and we will remove access to the work immediately and investigate your claim.

LUND UNIVERSITY

PO Box 117  
221 00 Lund  
+46 46-222 00 00



# A numerical model to simulate short-term beach and dune evolution

JIE ZHANG

FACULTY OF ENGINEERING | LUND UNIVERSITY





*A numerical model to simulate short-term beach and dune evolution*



# A numerical model to simulate short-term beach and dune evolution

Jie Zhang



**LUND**  
UNIVERSITY

DOCTORAL DISSERTATION

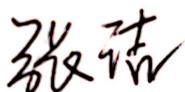
by due permission of the Faculty of Engineering, Lund University, Sweden.  
To be defended at the Faculty of Engineering, V-building, John Ericssons Väg 1,  
Lund, room V:C on May 28th, 2021 at 13:00.

*Faculty opponent*  
Prof. Dr. Ping Wang

<b>Organization</b> LUND UNIVERSITY Water Resources Engineering Box 118 SE-221 00 Lund, Sweden Author(s) Jie Zhang	<b>Document name</b> Doctoral Thesis, report TVVR-1090	
	<b>Date of issue</b> May 28th, 2021	
	Sponsoring organization China Scholarship Council (CSC)	
<b>Title and subtitle</b> A numerical model to simulate short-term beach and dune evolution		
<b>Abstract</b> <p>Sediment transport in the cross-shore (CS) and associated changes in the beach profile, especially during storms, have been topics of widespread concern. Since storms are often accompanied by high water levels and large waves, large quantities of sand from the beach and the dune are typically transported offshore, leading to severe beach and dune erosion, which threatens the integrity of buildings and infrastructure near the coast. With climate change, sea levels are expected to rise and storms are likely to grow in numbers and intensity, which further aggravates coastal flooding and erosion. The capability to quantify storm impact on the beach and dune is becoming increasingly important both for coastal engineers and managers.</p> <p>Thus, in this thesis, a new numerical model to simulate hydrodynamics, CS sediment transport, as well as beach and dune evolution under varying waves and water levels was developed. Particular focus was put on describing the response of the subaerial region of the profile, involving the foreshore, the berm, and the dune. A variety of modules, involving wave transformation, CS currents, mean water elevation, and CS sediment transport across the profile, by including relevant physics in combination with a set of theoretical and empirical formulas were included in the model.</p> <p>The theory employed in the new model was first calibrated and validated against data from the SUPERTANK laboratory, where the experimental cases selected encompassed several types of profile evolution, including berm erosion and bar formation, berm flooding and erosion, and offshore mound evolution. Good agreement was obtained between calculations and measurements, indicating that the model can produce robust and reliable predictions of CS transport and profile evolution in the nearshore.</p> <p>Then, the model was applied to two field sites, Cocoa Beach and Perdido Key Beach in Florida, USA, to simulate the evolution of a mound placed in the offshore exposed to varying non-breaking waves and water levels. In addition, several scenarios with different mound volume and location designs were investigated to indicate potential uses for the model. The results illustrate that the model can be used for providing guidance to the design of mounds in the offshore that is of great value in coastal planning and management, especially for beach nourishment.</p> <p>Finally, the model was applied to simulate the dune erosion during storms, where the wave impact theory was used for describing the impact of waves on the dune. Both laboratory data and field data were used for model testing. The results indicated that the model could reproduce the dune retreat rather well.</p> <p>Overall, the new numerical model could be a useful tool in practical engineering projects for predicting CS sediment transport and beach and dune profile evolution.</p>		
<b>Key words:</b> Numerical model, cross-shore transport, beach profile change, dune erosion, offshore mound, storms		
Classification system and/or index terms (if any)		
Supplementary bibliographical information		<b>Language:</b> English
<b>ISSN and key title</b> 1101-9824		<b>ISBN</b> 978-91-7895-875-7 (print) 978-91-7895-876-4 (pdf)
Recipient's notes	<b>Number of pages</b> 84	Price
	Security classification	

I, the undersigned, being the copyright owner of the abstract of the above-mentioned dissertation, hereby grant to all reference sources permission to publish and disseminate the abstract of the above-mentioned dissertation.

Signature



Date 2021-04-19

# A numerical model to simulate short-term beach and dune evolution

Jie Zhang



**LUND**  
UNIVERSITY

Coverphoto by Jie Zhang

Copyright pp 1-84 Jie Zhang, 2021

Paper 1 © Coastal Education & Research Foundation

Paper 2 © MDPI

Paper 3 © American Society of Civil Engineers

Paper 4 © by the Authors (Manuscript unpublished)

Paper 5 © by the Authors (Manuscript unpublished)

Faculty of Engineering

Department of Building and Environmental Technology

ISBN 978-91-7895-875-7 (print), 978-91-7895-876-4 (pdf)

ISSN 1101-9824

Printed in Sweden by Media-Tryck, Lund University  
Lund 2021



Media-Tryck is an environmentally  
certified and ISO 14001:2015 certified  
provider of printed material.  
Read more about our environmental  
work at [www.mediatryck.lu.se](http://www.mediatryck.lu.se)

**MADE IN SWEDEN** 

*To the people who are interested in my study*



# Table of Contents

	Acknowledgements .....	i
	Popular science summary .....	ii
	Abstract .....	iv
	摘要 .....	vi
	Papers .....	vii
	Appended papers .....	vii
	The author's contribution to the appended papers.....	vii
	Other related publications.....	viii
	List of symbols .....	ix
<b>1</b>	<b>Introduction .....</b>	<b>1</b>
	1.1 Background.....	1
	1.2 Objectives and procedure .....	2
	1.3 Thesis structure.....	3
<b>2</b>	<b>Model development .....</b>	<b>5</b>
	2.1 Theoretical background .....	5
	2.2 Model structure.....	6
	2.3 Model theory .....	8
	2.3.1 Wave transformation .....	8
	2.3.2 Cross-shore currents .....	9
	2.3.3 Shear stresses.....	10
	2.3.4 Sediment transport.....	11
	2.3.5 The effect of the long waves.....	17
	2.4 General insights into beach and dune evolution .....	20
	2.4.1 Storm impact mechanism .....	20
	2.4.2 The effects of longshore transport .....	21
<b>3</b>	<b>Model application.....</b>	<b>23</b>
	3.1 Beach profile evolution in the nearshore .....	23
	3.1.1 General description.....	23
	3.1.2 Data collection.....	24
	3.1.3 Model set up .....	24

3.1.4	Results .....	25
3.2	Mound evolution in the offshore .....	30
3.2.1	General description.....	30
3.2.2	Data collection.....	32
3.2.3	Model set up .....	34
3.2.4	Results .....	34
3.3	Dune evolution .....	44
3.3.1	General description.....	44
3.3.2	Data collection.....	45
3.3.3	Model set up .....	46
3.3.4	Results .....	47
<b>4</b>	<b>Discussion.....</b>	<b>53</b>
4.1	Model novelty.....	53
4.2	Model limitations and future improvements.....	54
<b>5</b>	<b>Conclusions .....</b>	<b>56</b>
<b>6</b>	<b>References .....</b>	<b>57</b>

# Acknowledgements

I would like to express my deepest gratitude to my supervisor Prof. Magnus Larson. Thanks for his patient guidance, valuable and constructive suggestions, and enthusiastic encouragement. He is a generous, intelligent, humorous, and friendly person, whom I admire the most and appreciate working with. I am so lucky to have him as my supervisor. Thanks to my co-supervisor Prof. Hans Hanson for leading me into the coastal world by providing me with the course of Coastal Hydraulics at the very beginning of my study.

I would also like to offer my special thanks to Prof. Linus Zhang for picking me up when I arrived in Sweden for the first time. Thanks for his warm, generous hospitality during special festivals, which makes me feel at home.

My grateful thanks are extended to Cintia Bertacchi Uvo, Magnus Persson, and Carina Littrén for providing a bright work environment, to Peder Hjorth, who taught me some Swedish and recommended me some interesting articles and books.

Thanks to all the people at TVRL. I am particularly grateful to Almir Nunes De Brito Junior for his help in programming, to Caroline Hallin for her valuable comments in paper IV.

I would like to express my very great appreciation to the China Scholarship Council (CSC) for supporting me to pursue a PhD, to ÅForsk and Åke och Greta Lissheds stiftelse for providing me the opportunities to conduct academic exchange and build a worldwide network with the people in my field.

I would also like to acknowledge my project partners, Yoshimitsu Tajima at the University of Tokyo and Fangfang Zhu at the University of Nottingham Ningbo China, for fruitful workshops with valuable feedback and warm hospitality during my visits.

Thanks to all my dearest friends, Jing Li, Cheng Qian, Yiheng Du, Yuchen Yang, Dong An, Han Yu, Yun Weng, Feifei Yuan, Zhenpeng Ge, Yajun Huang, Xinyi Zhang, Yuchen Jiang, Rui Shuai, Fang Liu, Qi Shi, Xianshao Zou, Zhengjun Wang, Juanzi Shi, Jun Li, Huiting Ma, Suxun Pan, Xiujuan Qiao, Xin Liu, Anchita, Sameh, Peter, Dauren, Shokoufeh, Shifteh, Mohammed, Denis, Carla, Claudia, Erik, Bárbara, Clemêncio. Thanks for your support and friendship. I am grateful to have you around.

I wish to thank my family for their endless love, support, and encouragement throughout my study. Thanks to my parents for always respecting my decision. Special thanks go to my husband, Gazi Zang, you are my strongest backing regardless of my ups and downs.

## Popular science summary

Sandy beaches constitute more than 30% of the world's coastlines (Luijendijk et al., 2018). They are not only popular recreational sites for people, but are also significant habitats for various marine species. Moreover, sandy beaches act as natural buffer areas against storms playing an important role in protecting infrastructure and property in the coastal region. Due to these characteristics, sandy beaches are highly developed and exploited by humans, which often affect the balance of coastal processes, resulting in severe beach erosion. Beach erosion is the removal of sediment from a particular coastal area driven by waves, currents, and wind. In the past, beach erosion was typically a continuing natural process. Today, it is often the result of human activities, becoming headline issues around the world when it appears.

At present, around 70% of the sandy beaches are subjected to erosion in the world (Anthony, 2005; Bird, 1996) and this situation is getting worse due to climate change. With climate change, sea levels are expected to rise and storms are projected to occur more frequently and to intensify. Sea level rise increases the probability of beach flooding and erosion. Storms are often associated with high water levels and large waves that may cause a series of potential hazards, threatening the integrity of the beach system. According to a recent study (Vousdoukas et al., 2020), 50% of the world's beaches could disappear by the end of this century.

Facing such severe erosion problems, preventing sandy beaches from eroding is of great urgency, posing a considerable challenge. To address such problems, the capability to quantify storm impact on sandy beaches is of great significance for coastal safety and sustainable development. Although there are a number of empirical and numerical models to quantitatively understand the morphological change of sandy beaches to different types of forcing in time and space, most of them have a focus on specific regions of the beach using rather limited data for model validation, especially in the subaerial region, but also with regard to field cases. Therefore, in the present study, a numerical model to simulate beach and dune evolution due to cross-shore transport under varying waves and water levels was developed with a special emphasis on the subaerial region.

The main purpose of this model was to describe the physical processes along the entire beach profile and the interconnection among the different regions, and then to predict the beach and dune morphological change with time. The model was developed and applied to cases with different characteristics, including berm flooding and erosion, bar formation, offshore mound evolution, as well as dune erosion; the simulation results showed satisfactory agreement compared to measured data.

In conclusion, the model is robust and reliable in simulating beach and dune evolution as well as cross-shore sediment transport, and can serve as a powerful tool for assisting engineers and managers in coastal protection and management.

# Abstract

Sediment transport in the cross-shore (CS) and associated changes in the beach profile, especially during storms, have been topics of widespread concern. Since storms are often accompanied by high water levels and large waves, large quantities of sand from the beach and the dune are typically transported offshore, leading to severe beach and dune erosion, which threatens the integrity of buildings and infrastructure near the coast. With climate change, sea levels are expected to rise and storms are likely to grow in numbers and intensity, which further aggravates coastal flooding and erosion. The capability to quantify storm impact on the beach and dune is becoming increasingly important both for coastal engineers and managers.

Thus, in this thesis, a new numerical model to simulate hydrodynamics, CS sediment transport, as well as beach and dune evolution under varying waves and water levels was developed. Particular focus was put on describing the response of the subaerial region of the profile, involving the foreshore, the berm, and the dune. A variety of modules, involving wave transformation, CS currents, mean water elevation, and CS sediment transport across the profile, by including relevant physics in combination with a set of theoretical and empirical formulas were included in the model.

The theory employed in the new model was first calibrated and validated against data from the SUPERTANK laboratory, where the experimental cases selected encompassed several types of profile evolution, including berm erosion and bar formation, berm flooding and erosion, and offshore mound evolution. Good agreement was obtained between calculations and measurements, indicating that the model can produce robust and reliable predictions of CS transport and profile evolution in the nearshore.

Then, the model was applied to two field sites, Cocoa Beach and Perdido Key Beach in Florida, USA, to simulate the evolution of a mound placed in the offshore exposed to varying non-breaking waves and water levels. In addition, several scenarios with different mound volume and location designs were investigated to indicate potential uses for the model. The results illustrate that the model can be used for providing guidance to the design of mounds in the offshore that is of great value in coastal planning and management, especially for beach nourishment.

Finally, the model was applied to simulate the dune erosion during storms, where the wave impact theory was used for describing the impact of waves on the dune. Both laboratory data and field data were used for model testing. The results indicated that the model could reproduce the dune retreat rather well.

Overall, the new numerical model could be a useful tool in practical engineering projects for predicting CS sediment transport and beach and dune profile evolution.

## 摘要

风暴作用下的跨岸泥沙输移以及沙滩剖面演化，一直以来都是广泛关注的话题。风暴通常伴随着高水位和巨大的波浪，导致沙滩和沙丘上的大量泥沙向离岸方向输移，对沙滩和沙丘产生严重的侵蚀，威胁着沿海建筑和基础设施的完整性。随着气候变化，预计海平面上升，风暴数量和强度可能会增加，这将进一步加剧沿海洪水和侵蚀的发生。对海岸工程师和管理人员而言，量化风暴对沙滩和沙丘的影响变得尤其重要。

因此，本文致力于开发一个新的数值模型，用来模拟不同波浪和水位作用下，海岸水动力，跨岸泥沙输移以及沙滩和沙丘的演化。本研究侧重于描述沙滩剖面的水上区域，包括前滨，堤岸和沙丘。该模型包含波浪变换、跨岸流、平均水位以及跨岸泥沙输移等模块，将不同模块相关的物理过程与一系列的理论和经验公式相结合。

本研究首先采用美国超级水槽 (SUPERTANK) 实验数据对模型进行校核和验证。此过程选取了超级水槽实验中不同类型的沙滩剖面案例，包括堤岸侵蚀和沙坝形成、堤岸淹没侵蚀以及离岸沙丘的演化。计算结果和实验测量数据吻合良好，表明该模型可为近海跨岸泥沙输移和沙滩剖面演化提供可靠的预测。

接下来，该模型被用于模拟在变化的非破碎波和水位作用下，美国佛罗里达 Cocoa 沙滩以及 Perdido Key 沙滩深水区的离岸丘的演化。此外，为了进一步测试模型的性能，进行了不同离岸丘体积以及不同放置位置场景的设计。研究表明，模型对模拟不同场景下的离岸丘的演化具有潜力。由此可见该模型可以对离岸丘的设计提供指导，对海岸规划和管理，特别是沙滩的补给，具有重要的价值。

最后，该模型被用于模拟风暴作用下沙丘的侵蚀，其中波浪冲击理论用于描述波浪对沙丘的影响。实验数据和现场数据被同时用于模型的测试。结果表明，该模型可以较好的模拟沙丘的侵蚀撤退。

总之，新的数值模型可作为有用的工具被应用于实际的工程项目中，用来预测跨岸沉积物的输移以及沙滩和沙丘剖面的演化。

# Papers

## Appended papers

The thesis is based on the following papers which are referred to by their Roman numerals in the body of the text.

- I. **Zhang, J.**, Larson, M. and Ge, Z.P., 2020. Numerical model of beach profile evolution in the nearshore. *Journal of Coastal Research*, 36(3): 506-520. <https://doi.org/10.2112/JCOASTRES-D-19-00065.1>.
- II. **Zhang, J.** and Larson, M., 2020. A numerical model for offshore mound evolution. *Journal of Marine Science and Engineering*, 8(3): 160. <https://doi.org/10.3390/jmse8030160>.
- III. **Zhang, J.** and Larson, M. Simple methods for direct computation of bed roughness due to sediment transport. *Journal of Hydraulic Engineering*, accepted.
- IV. **Zhang, J.** and Larson, M. Decadal-scale subaerial beach and dune evolution at Duck, North Carolina. *Marine Geology*, under revision.
- V. **Zhang, J.** and Larson, M. A numerical model to simulate beach and dune evolution. Submitted to *Journal of Coastal Research*.

## The author's contribution to the appended papers

- I. The author contributed to the theoretical discussions, data compilation, the model development and testing, and wrote the manuscript.
- II. The author contributed to the compilation and analysis of field cases, the model implementation and application, and wrote the manuscript.
- III. The author contributed to the theoretical discussions and wrote the manuscript.
- IV. The author contributed to the data compilation, the statistical analysis, the discussion of the results, and wrote the manuscript.
- V. The author contributed to the model development, data compilation, the model application, and wrote the manuscript.

## Other related publications

**Zhang, J.**, Larson, M. and Ge, Z., 2018. A model to simulate beach profile evolution induced by storms. *Coastal Engineering Proceedings*, (36): 10-10.

**Zhang, J.**, Larson, M. and Hallin, C., 2019. Decadal-scale dune evolution at Duck, North Carolina. *Coastal Sediments 2019*, pp. 1365-1372.

## List of symbols

$a$	Empirical coefficient in the equation to determine the friction factor
$a_c$	Empirical coefficient in determining bed load due to undertow
$a_w$	Empirical coefficient related to the generalized bed load formula
$A_w$	Horizontal bottom wave excursion amplitude
$b$	Empirical coefficient related to the generalized bed load formula
$B$	A parameter related to the wave shape
$C$	Wave phase speed
$C_E$	Empirical coefficient related to the weight of dune erosion
$C_g$	Wave group speed
$c_R$	A reference concentration at the bed
$C_u$	Empirical coefficient in determining the speed of the swash bore
$d$	Total water depth
$d_{50}$	Median grain size
$d_c$	Distance from the trough level to crest level
$d_t$	Distance from the bed to trough level
$f$	Friction factor
$F$	Swash force
$f_c$	Friction factor for current
$F_o$	Swash force for a single bore
$F_{rms}$	Wave energy flux
$F_{stab}$	Stable wave energy flux
$f_w$	Friction factor for waves
$g$	Acceleration due to gravity
$H$	Wave height
$H_{mean}$	Mean breaking wave height
$H_n$	Rms wave height for non-breaking waves
$h_o$	Height of the bore

$H_{rms}$	Rms wave height for breaking and non-breaking waves
$H_{rmso}$	Rms wave height in deep water
$H_x$	Rms wave height at location $x$ ignoring breaking
$k_1$	Empirical coefficient related to the undertow velocity
$k_2$	Empirical coefficient related to the undertow velocity
$K_a$	A function only of the Ursell number
$K_c$	Empirical coefficient related to swash-zone transport rate
$k_s$	Nikuradse roughness
$k_{s,g}$	Roughness due to skin friction
$k_{s,r}$	Roughness due to bed forms
$k_{s,sf}$	Roughness due to sediment transport
$L$	Local wavelength
$L_o$	Wave length in deep water
$m_o$	Mass of the bore
$n$	Number of values
$p$	Porosity
$q_b$	Net transport rate during a wave cycle
$q_{ba}$	Sediment transport during a wave cycle due to asymmetry
$q_{bs}$	Net swash-zone sediment transport rate over a cycle
$q_{bu}$	Bed load transport due to undertow
$q_D$	Average rate of dune erosion
$q_{sb}$	Sediment transport rate from trough level to crest level
$q_{su}$	Sediment transport rate from the bed to trough level
$r$	Relative roughness
$R$	Runup height (estimated by a Hunt-type runup formula)
$R_L$	Total runup height
$R_{Lp}$	Total runup height for different values on exceedance probability
$R_p$	Runup height corresponding to a certain exceedance
$R_{rms}$	Rms runup height obtained from the Hunt formula

$s$	Specific gravity of the sediment
$s_o$	Length of the swash bore
$T$	Swash period (assumed equal to the wave period)
$T_c$	Duration for the onshore phase
$t_o$	Duration of the swash at the particular location
$t_s$	Arrival time of the uprush at a particular location
$T_t$	Duration for the offshore phase
$\hat{u}$	Equal to the sum of $u_c$ and $u_t$
$u$	Instantaneous horizontal bottom orbital velocity
$U$	Water velocity
$U_b$	Mean velocity above trough level
$u_c$	Peak onshore velocity
$u_{linear}$	Peak near-bed horizontal velocity using linear wave theory
$U_m$	Mean velocity below trough level
$u_o$	Wave front speed at uprush
$U_r$	Ursell number
$u_s$	Wave front speed at the beginning of uprush
$u_t$	Peak offshore velocity
$U_w$	Wave velocity
$V_o$	Initial volume of the dune
$w_s$	Sediment fall speed
$y_{0i}$	Initial bed elevation
$z_0$	Bed roughness length
$z_o$	Elevation difference between dune foot and the beginning of swash
$\alpha$	Ratio of breaking waves
$\Gamma$	Empirical coefficient in determining the stable wave energy flux
$\Gamma$	Incomplete function
$\delta$	Ratio between long-wave amplitude and short-wave runup height
$\Delta t$	A period of time

$\Delta V$	Eroded volume
$\Delta W$	Weight of the eroded volume
$\Delta y_m$	Error in measured bed elevation in SUPERTANK
$\varepsilon$	Sediment diffusivity
$\theta$	Shields parameter
$\theta_{cr}$	Critical Shields parameter
$\theta_{cw}$	Maximum Shields parameter due to currents and waves
$\theta_{cw,m}$	Mean Shields parameter due to currents and waves
$\theta_w^{net}$	Net Shields parameter during a wave cycle
$\theta_w$	Instantaneous Shields parameter
$\kappa$	Von Karman constant
$\rho$	Water density
$\rho_s$	Sediment density
$\tau_b$	Bed shear stress
$\varphi$	Incident wave angle
$\Psi$	Empirical function characterizing the shape of the temporal velocity
$\gamma_b$	Breaker depth ratio for an individual wave
$\beta_e$	Local equilibrium slope
$\phi_m$	Friction angle for a moving grain (about 30 deg)
$\eta_L$	Long-wave amplitude

# 1 Introduction

*This chapter outlines the general problems that motivated the author to carry out this thesis study, as well as the main goals to be achieved. In addition, the thesis structure and the interconnection among the appended papers are briefly described.*

## 1.1 Background

Currently, nearly 2.4 billion people (around 40% of the world's population) live within 100 km of the coast (United Nations, 2017). Due to the high population pressure, the utilization of sandy beaches for human activities such as recreation, human development and habitation has constantly been increasing, which in turn aggravates the vulnerability of coastal areas and has tremendous impacts to the coastal ecosystems. Thus, concern over the condition of sandy beaches has always been a hot topic.

In addition, due to climate change, sea levels are expected to rise and storms are likely to grow in numbers and intensities. Sea level rise increases the probability of beach flooding and erosion. Storms are often accompanied by high water levels (surge) and large waves that erode the berm and dune, carrying large quantities of sand offshore, causing severe damage to buildings, infrastructure, and other features of values behind the beach system. Thus, the capability to quantify storm impact on beach profiles is becoming increasingly significant for coastal zone management in predictions, analysis, and design.

In order to tackle this problem, numerical models have been developed as powerful tools to predict the beach profile change induced by cross-shore (CS) sediment transport. However, the interactions between currents, wave, sediment transport, and beach profile change are complex and nonlinear. Because of the complexity of the governing processes, simplifications are required in terms of deriving the equations for describing those processes. In other words, extensive models for predicting beach profile evolution either rely on empirical or semi-empirical formulae that require confirmation through experimental data. It should also be noted that such models often need more detailed data of high quality to meet satisfactory agreement.

Furthermore, previous models for quantitative predictions mainly focused on certain morphological features of beach profile change, such as bar or berm formation and dune erosion in time and space under specific wave and current conditions. However, the beach profile can be divided into different zones, encompassing the dune, swash, surf and offshore zone. Even if in previous model development attempted to focus on the evolution of the entire beach profile, the existing models typically emphasize particular zones and treat the other zones in a rather schematic manner, where the connection to the main governing processes is more limited. Therefore, developing a physical-based model to simulate the response of the entire beach profile to varying waves and currents that can be employed in practical projects is of importance for coastal engineers and managers.

## 1.2 Objectives and procedure

The overall objective of this thesis is to develop a robust and reliable model to simulate the entire beach profile evolution due to varying waves and water levels. A key point is to reproduce the beach change based on physical descriptions of the governing processes in the different regions of the profile, including the offshore, surf, swash, and dune zone. Also, the model should be extensively validated with measurements from both the laboratory and the field to make it applicable in practical engineering projects. In order to achieve this objective, the process of model development was divided into the following steps.

1. Perform a review of relevant literature on beach profile evolution during storms and its mathematical modelling. Summarize observed problems concerning simulating sediment transport and resulting erosion and accretion, especially in the subaerial portion of the beach profile.
2. Compile available data sets on beach profile change in the open literature of relevance for the present modeling.
3. Formulate governing equations concerning CS sediment transport and profile response, both for the subaerial and subaqueous portion of the profile, and test them against available data.
4. Develop a general model of profile evolution that couples the CS sediment transport model with a hydrodynamic model of wave transformation in the nearshore area, and test it with available data.
5. Integrate the different modules for CS transport, swash transport, berm-dune interaction, nearshore-offshore interaction, and profile recovery into a complete profile evolution model and simulate coastal evolution for compiled data sets to validate the model.

## 1.3 Thesis structure

This thesis is based on a summary that is related to the five appended papers. A brief description of the appended papers and their interconnection is presented below:

**Paper I** presents the development of a numerical model including various modules for beach profile evolution in the nearshore due to varying waves and water levels. However, modules for dune erosion has not yet been integrated into the model.

In **Paper II**, the model developed in **Paper I** is applied to investigate the mound evolution in the offshore over long time periods.

In **Paper III**, the theories about bed roughness computation due to sediment transport employed in **Paper I** are described in detail and constructed to a technical note.

**Paper IV** analyses the temporal and spatial characteristics of beach and dune morphology evolution at Duck, North Carolina in recent decades based on a range of statistical methods. The main purpose of **Paper IV** is to identify the important factors governing the beach and dune evolution, which not only provides general insights on beach and dune morphology change, but also contributes to the development of the dune module carried out in **Paper V**.

Finally, in **Paper V**, the module for dune erosion is coupled to the current model and a complete model for beach profile evolution is developed.

The thesis is structured as follows. **Chapter 2** presents the model development, including the theoretical background, model structure, and model theory. **Chapter 3** describes the model application. **Chapter 4** discusses the model novelty, model limitations, and future improvements. Finally, conclusions and references are given in **Chapter 5** and **Chapter 6** respectively.



## 2 Model development

*This chapter first presents the theoretical background to the model by performing a review of relevant literature. Then the structure of the model and the specific theoretical approaches are described. Lastly, general insights into the morphological behaviour of beaches and dunes are presented.*

### 2.1 Theoretical background

In the earliest models for quantitative predictions of beach morphology, the focus was mainly put on certain properties of beach profile change. For example, whether a bar or berm would form under certain governing factors (waves and sand characteristics), and what are the relationships between the governing factors and the profile response. Meanwhile, various empirical equations have been derived based on laboratory experiments (Bagnold, 1940; Iwagaki and Noda, 1962; Kajima, 1983; Kraus and Larson, 1988; Watts and Dearduff, 1954) or field measurements (Bascom, 1951; King and Williams, 1949; Owens, 1977; Wright et al., 1986).

Since the 1980s, a variety of numerical models of beach profile change have been developed. However, just a few of the numerical models have been frequently used for engineering predictions. For instance, the model (EBEACH) to simulate the beach profile change with focus on dune erosion proposed by Kriebel and Dean (1985) was the most successful and widely used numerical model in the earliest period. The model was based on the concept of an equilibrium beach profile (EBP) and the CS transport rate was calculated according to the deviation between the actual profile and the EBP. However, features such as bars and berms are not incorporated in the model, and beach accretion is not simulated quantitatively. Larson and Kraus (1989) developed an empirically based model (SBEACH) to calculate beach and dune erosion under storms applying the EBP concept. SBEACH is applicable to describe the development of bars and berms under the assumption that the major morphologic change occurring in and around the surf zone under breaking waves. In other words, SBEACH could not simulate the sediment transport in the offshore with nonbreaking waves.

Subsequently, a large number of process-based CS profile evolution models have emerged, such as CIRRC (Rivero and S-Arcilla, 1993), COSMOS (Southgate and Nairn, 1993), UNIBEST (Reniers et al., 1995), CROSMOR (Van Rijn and Wijnberg, 1996), and BEACH (O'Connor et al., 1998). Although the profile models can reasonably produce the behaviour of the outer bar system on the time scale of storms and seasons, they are not suitable for detailed simulating the foreshore and dune region on a seasonal time scale (Van Rijn et al., 2003). Steetzel (1990) attempted to develop a model DUROSTA to simulate the profile change with a special focus on the dune, the model is only limited to predict the dune erosion as a large volume under a known storm surge. Ruessink et al. (2007) presented a numerical model for simulating sandbar migration of the subaqueous region. Jayaratne et al. (2014) developed a two-dimensional beach profile evolution model for describing onshore-offshore sand bar migration but the swash dynamics was not incorporated in the model.

From a CS sediment transport point of view, the entire beach profile can be divided into different zones, including the dune, swash, surf, and offshore zone. Most of the above models have a focus on specific regions of the beach rather than the entire beach. Therefore, it may be difficult to accurately predict bed morphology change along the entire beach profile over different time scales using these models.

In recent models, more efforts have been made to predict the evolution along the entire profile, i.e., both in the subaerial and subaqueous regions. Johnson et al. (2012) developed a CS model (CSHORE) to simulate beach erosion under combined effect of waves and currents, but some improvements are needed in determining the sediment transport and morphology evolution in the intermittently wet zone. At present, the model XBeach developed by Roelvink et al. (2009) is the most popular and widely used model in simulating the entire beach response. XBeach, as a two-dimensional process-based model, is well capable of describing long-wave motions created by short-wave group, but the description of the dune region is based on an avalanching scheme, which is much more ad hoc and typically validated with limited data.

In terms of existing models, a full description of the mechanism in sediment transport and beach profile evolution has not reached a satisfactory level. Therefore, this thesis aims at developing a better understanding of all phenomena along the entire beach profile and develop a new physically-based profile evolution model that can not only predict the entire beach morphology change based on theoretical concepts, but can also be utilized for practical projects.

## 2.2 Model structure

In the present study, the model encompasses a number of modules for describing the hydrodynamic and morphodynamic processes based on different theoretical and empirical formulae that have been extensively validated with data. The hydrodynamic processes describe wave transformation, mean CS currents, and mean water elevation. The morphodynamic processes calculate the CS sediment transport in different beach regions, avalanching, and sand volume conservation. The connections among the different modules are presented in Figure 1.

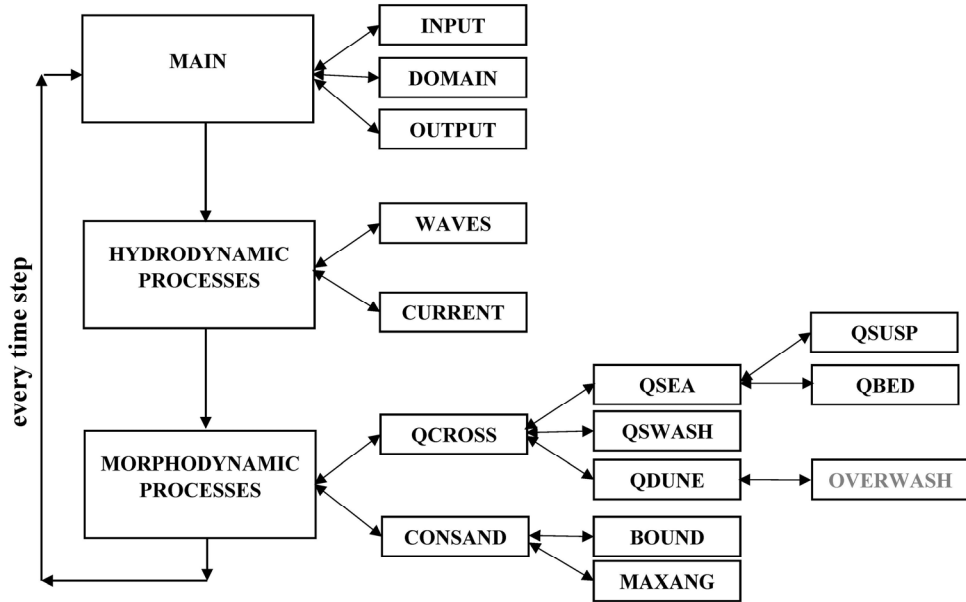


**Figure 1. Schematic of the connections among the various calculation modules in the numerical model of beach profile evolution.**

The MAIN module controls the calculations in different regions of the beach identified through DOMAIN by giving the input data obtained from INPUT, involving the initial profile, general parameters, wave conditions, and water levels, whereas the simulated results are saved in OUTPUT. WAVES is associated with the CS wave transformation employing a random breaker decay model based on linear wave theory. In parallel with using the wave transformation equation, the mean water elevation, e.g., wave setup/setdown can be obtained by solving the CS momentum equation. CURRENT determines the mean CS current. QCROSS calculates CS sediment transport in different regions, involving offshore and surf zone (QSEA), swash zone (QSWASH), as well as dune (QDUNE), whereas QSEA consists of suspended load transport (QSUSP) and bed load transport (QBED). OVERWASH has not yet been integrated into the present model. CONSAND updates the profile elevations by solving the sand volume conservation equation under the given boundary conditions (BOUND). MAXANG is applied to check for

avalanching if the local slopes are too steep. In the model, the calculations of waves, currents, sediment transport, and profile elevations are performed at every time step.

## 2.3 Model theory

In this part, the theoretical formulations employed in different modules, such as wave transformation, CS currents, and CS sediment transport including shear stresses, are introduced. In addition, in order to make the model applicable for simulating beach profile evolution induced by long waves, an improved method to estimate the runup is described as well.

### 2.3.1 Wave transformation

The model for decay of random waves developed by Larson (1995) is employed for the wave transformation. This model relies on the equation proposed by Dally et al. (1985) that requires transformation of only the root-mean-square (rms) wave height without making any assumption about the shape of the probability density function. A wave-by-wave approach that involves transformation of many individual waves characterized by a Rayleigh distribution is employed.

Assuming that the energy dissipation is related to depth-dependent wave breaking, the energy conservation equation is expressed as,

$$\frac{d}{dx}(F_{rms} \cos \varphi) = \frac{\kappa}{d}(F_{rms} - F_{stab}) \quad (1)$$

where  $F_{rms}$  is the wave energy flux;  $\varphi$  is the incident wave angle;  $\kappa$  is an empirical coefficient;  $d$  is the total water depth; and  $F_{stab}$  is the stable wave energy flux. According to linear wave theory, the energy flux  $F_{rms}$  can be given by,

$$F_{rms} = \frac{1}{8} \rho g H_{rms}^2 C_g \quad (2)$$

In which  $\rho$  is the water density;  $g$  is the acceleration due to gravity;  $H_{rms}$  is the rms wave height for breaking and non-breaking waves; and  $C_g$  is the wave group speed. The stable wave energy flux  $F_{stab}$  can be written for random waves,

$$F_{stab} = \frac{1}{8} \rho g ((1 - \alpha) H_n^2 + \alpha \Gamma^2 d^2) C_g \quad (3)$$

where  $\alpha$  is the ratio of breaking waves;  $H_n$  is the rms wave height for non-breaking waves; and  $\Gamma$  is an empirical coefficient. According to Dally (1990), the ratio of breaking waves at a location  $x$  may be determined by,

$$\alpha = \exp\left(-(\gamma_b d / H_x)^2\right) \quad (4)$$

where  $\gamma_b$  is the breaker depth ratio for an individual wave; and  $H_x$  is the rms wave height at location  $x$  ignoring breaking. The rms wave height for non-breaking waves can be derived from the truncated Rayleigh distribution,

$$H_n^2 = \left(H_x^2 - \alpha(H_x^2 + \gamma_b^2 d^2)\right) / (1 - \alpha) \quad (5)$$

where  $\alpha$  and  $H_n$  are applicable for a monotonic profile and can be calculated explicitly at each point across shore. For a non-monotonic beach profile, such as a barred profile, waves that are reforming need to be involved in the calculation of  $\alpha$  and  $H_n$ ; the details are further discussed in Larson (1995). By solving Eqs. (1) - (5),  $H_{rms}$  can be calculated at all locations along the profile. The wave angle is determined by Snell's law. In parallel with solving the wave transformation equation, the CS momentum equation is solved to yield the mean water elevation.

### 2.3.2 Cross-shore currents

The return current, also denoted as undertow, which is induced both by the breaking waves and the Stokes drift, is of great significance in calculating the CS sediment transport. The mean velocity of the undertow for monochromatic waves developed by Rattanapitikon and Shibayama (2000) is,

$$U_m = k_1 \frac{BgH^2}{Cd_t} + k_2 \frac{BCH}{d_t} \quad (6)$$

where  $B$  is a parameter related to the wave shape;  $H$  is the wave height;  $C$  is the wave phase speed;  $d_t$  is the distance from the bed to trough level;  $k_1 = 0.76$  and  $k_2 = 1.12$  are coefficients. For the case of random waves, Eq. (6) can be generalized based on a wave-by-wave approach to yield,

$$U_m = k_1 \frac{BgH_{rms}^2}{Cd_t} + k_2 \frac{BCH_{mean}}{d_t} \alpha \quad (7)$$

where  $H_{rms}$  is the root-mean-square wave height for all waves;  $H_{mean}$  the mean breaking wave height that can be expressed as:

$$H_{mean} = (\alpha\Gamma + (1 - \alpha)\gamma_b)d \quad (8)$$

The onshore current above trough level is balanced by the undertow and can easily be determined based on the continuity equation.

### 2.3.3 Shear stresses

The shear stresses that may be induced by currents, waves, or combined wave-current (Soulsby, 1997), play a vital role in calculating the CS sediment transport. In general, the bed shear stress under a uniform current is determined by,

$$\tau_b = \frac{1}{2} \rho f U^2 \quad (9)$$

in which  $U$  is the water velocity; and  $f$  is the friction factor.

For the current-related shear stress, the friction factor in Eq. (9) can be derived by assuming a logarithmic velocity profile (Soulsby, 1997),

$$f_c = 2\kappa^2 \left( 1 + \ln \left( \frac{z_o}{d} \right) \right)^{-2} \quad (10)$$

where the subscript  $c$  denotes current;  $\kappa$  ( $= 0.4$ ) is the von Karman constant; and  $z_o$  is the bed roughness length, which for rough turbulent flow can be obtained from,

$$z_o = k_s / 30 \quad (11)$$

where  $k_s$  is the Nikuradse roughness.

For the wave-related shear stress, the friction factor is estimated from Swart (1974),

$$\begin{aligned} f_w &= 0.3 & r &\leq 1.57 \\ f_w &= a \exp(b r^{-0.19}) & r &> 1.57 \end{aligned} \quad (12)$$

where the subscript  $w$  denotes wave;  $a = 0.00251$ ,  $b = 5.21$ ; and  $r$  is the relative roughness given by,

$$\begin{aligned} r &= A_w / k_s \\ A_w &= U_w T / 2\pi \end{aligned} \quad (13)$$

where  $T$  is the wave period;  $U_w$  is the wave velocity; and  $A_w$  is the horizontal bottom wave excursion amplitude.

Thus, the friction factors  $f_c$  and  $f_w$  can be computed if  $k_s$  is known. In general, the total bed roughness  $k_s$  is estimated as the linear sum of three contributions (Grant and Madsen, 1982; Nielsen, 1981; Xu and Wright, 1995), consisting of the roughness due to skin friction ( $k_{s,g}$ ), bed forms ( $k_{s,r}$ ), and sediment transport ( $k_{s,sf}$ ).

Roughness due to skin friction is expressed as,

$$k_{s,g} = 2d_{50} \quad (14)$$

in which  $d_{50}$  is the median grain size.

In order to calculate the roughness induced by bed forms ( $k_{s,r}$ ), the formulas proposed by van Rijn (1984) for waves and Soulsby (1997) for currents are used.

The roughness resulting from the motion of sediment is computed from the formula given by Wilson (1989),

$$k_{s,sf} / d_{50} = 5\theta \quad (15)$$

where  $\theta$  is the Shields parameter defined as,

$$\theta = \tau_b / ((\rho_s - \rho)gd_{50}) \quad (16)$$

in which  $\tau_b$  is the bed shear stress; and  $\rho_s$  is the sediment density. It should be noted that the bed roughness due to sediment transport cannot be solved explicitly since the bed roughness is related to the Shields parameter, which is unknown. In this case, an iterative approach is usually employed; however, it may require substantial computations.

In order to predict the bed roughness due to sediment transport in an efficient and accurate manner, simple methods for direct computation of bed roughness are employed. The methods yield approximate non-dimensional expressions for the exact solutions in terms of polynomials determined by least-square fits. The accuracy of the polynomials is quite high, with coefficients of determination of over 99%. The simple methods can reduce the execution time significantly, which has great applicability in the numerical models, especially for large-scale and long-term simulations. The details about the new approaches that allow for direct computation of the bed roughness due to sediment transport are described in **Paper III**.

Finally, the total roughness ( $k_s$ ) is simply computed as:

$$k_s = k_{s,g} + k_{s,r} + k_{s,sf} \quad (17)$$

Regarding the combined wave-current shear stress, the total friction factor  $f_{cw}$  is determined from a weighted value between  $f_c$  and  $f_w$  following Camenen and Larson (2005).

### 2.3.4 Sediment transport

After calculating the CS variation in the wave and current properties, the CS sediment transport in different regions, including offshore and surf zone, swash zone, as well as dune zone are determined, as described in detail below.

#### 2.3.4.1 Offshore and surf zone transport

In the offshore and surf zone, the CS sediment transport is mainly determined by bed load and suspended load. Contribution to the bed load stems from undertow and

wave asymmetry, whereas the suspended load is caused by the CS currents, e.g., onshore current and offshore current (undertow).

### *Bed load transport*

As mentioned before, the bed load transport is associated with two components, including wave asymmetry and undertow, which correspond to onshore transport and offshore transport, respectively. According to Camenen and Larson (2005), the generalized bed load formula is expressed as,

$$\frac{q_b}{\sqrt{(s-1)gd_{50}^3}} = a_w \sqrt{\theta_w^{net}} \theta_{cw,m} \exp\left(-b \frac{\theta_{cr}}{\theta_{cw}}\right) \quad (18)$$

in which  $q_b$  is the net transport rate during a wave cycle;  $s$  ( $= \rho_s/\rho$ ) is the specific gravity of the sediment;  $a_w$  ( $= 6$ ) and  $b$  ( $= 4.5$ ) are empirical coefficients;  $\theta_{cw,m}$  and  $\theta_{cw}$  are the mean Shields parameter and maximum Shields parameter due to currents and waves, respectively;  $\theta_{cr}$  is the critical Shields parameter; and  $\theta_w^{net}$  is the net Shields parameter during a wave cycle determined by,

$$\theta_w^{net} = \frac{1}{T} \left( \int_0^{T_c} \theta_w^{on} dt + \int_{T_c}^T \theta_w^{off} dt \right) \quad (19)$$

where  $T_c$  is period during which the flow is onshore; *on* and *off* are the phase of the wave cycle when the flow is onshore and offshore, respectively; and  $\theta_w$  is the instantaneous Shields parameter given by,

$$\theta_w = (f_w u^2) / (2(s-1)gd_{50}) \quad (20)$$

in which  $u$  is the instantaneous horizontal bottom orbital velocity. For describing the wave asymmetry, two sinusoidals are introduced to estimate the velocity variation during a wave cycle (Grasmeijer and Ruessink, 2003), together with peak velocities  $u_c$  and  $u_t$  (duration  $T_c$  and  $T_t$ , where  $T = T_c + T_t$ ) for the onshore and offshore phase, respectively. After integrating Eq. (19) by using Eq. (20), the net Shields parameter over a wave cycle is obtained:

$$\theta_w^{net} = \frac{1}{4(s-1)gd_{50}} \left( u_c^2 \frac{T_c}{T} - u_t^2 \frac{T_t}{T} \right) \quad (21)$$

According to the condition for continuity during a wave cycle,  $T_c$  and  $T_t$  can be denoted by:

$$\begin{aligned} T_c &= T u_t / (u_c + u_t) \\ T_t &= T u_c / (u_c + u_t) \end{aligned} \quad (22)$$

Substituting Eq. (22) into Eq. (21) and rearranging yield:

$$\theta_w^{net} = \frac{1}{4} \frac{f_w u_c^2}{(s-1)gd_{50}} \frac{T_c}{T} \left(1 - \frac{T_c}{T_t}\right) \quad (23)$$

Substituting Eq. (23) into Eq. (18) leads to,

$$q_{ba} = a_w \sqrt{\frac{f_w}{2}} d_{50} \hat{u} K_a \theta_{cw,m} \exp\left(-b \frac{\theta_{cr}}{\theta_{cw}}\right) \quad (24)$$

where,

$$K_a = \frac{u_c}{\hat{u}} \left( \frac{1}{2} \frac{T_c}{T} \left(1 - \frac{T_c}{T_t}\right) \right)^{1/2} \quad (25)$$

in which  $\hat{u} = u_c + u_t$ . Based on Grasmeijer and Ruessink (2003),  $\hat{u}$  can be determined by,

$$\hat{u} = 2ru_{linear} \quad (26)$$

where  $u_{linear}$  is the peak near-bed horizontal velocity computed using linear wave theory; and  $r$  is given by:

$$r = 1 - 0.4H / d \quad (27)$$

In order to calculate  $K_a$ , a wave theory is required to predict the wave quantities, i.e.,  $u_c$ ,  $u_t$ ,  $T_c$ , and  $T_t$  as shown in Eq. (25). Here, the first-order cnoidal wave theory is employed (Isobe, 1985) and it is found that  $K_a$  is a function only of the Ursell number ( $U_r$ ), where  $U_r = HL^2/d^3$  ( $H$  and  $L$  are the local wave height and wavelength, respectively). For the purpose of fast calculation of  $K_a$ , an empirical expression of polynomial type is developed by least-square fitting to cnoidal wave theory. In terms of the details of the methods for polynomials fitting can be found in **Paper II**. Thus, the sediment transport during a wave cycle due to asymmetry can be computed by substituting  $K_a$  into Eq. (24).

Bed load transport due to undertow is always offshore and can be obtained by combining Eq. (18) with the mean current at the bed resulting in,

$$q_{bu} = a_c \sqrt{\frac{f_c}{2}} d_{50} U_m \theta_{cw,m} \exp\left(-b \frac{\theta_{cr}}{\theta_{cw}}\right) \quad (28)$$

where  $a_c$  is an empirical coefficient. Finally, the net bed load transport is derived from the linear sum of the contribution to the bed load transport from wave asymmetry and undertow.

### *Suspended load transport*

The suspended load transport is determined by integrating the product between the flow velocity and sediment concentration (Nielsen, 1992). According to Camenen and Larson (2008), the sediment concentration distribution is well described by an exponential function expressed as,

$$c(z) = c_R \exp\left(-\frac{w_s z}{\varepsilon}\right) \quad (29)$$

where  $c_R$  is a reference concentration at the bed ( $z = 0$ );  $w_s$  is the sediment fall speed; and  $\varepsilon$  is the sediment diffusivity.

Integrating the sediment transport rate from the bed to the trough level leads to,

$$q_{su} = \int_0^{d_t} U_m c_R \exp\left(-\frac{w_s}{\varepsilon} z\right) dz = \frac{U_m c_R \varepsilon}{w_s} \left(1 - \exp\left(-\frac{w_s}{\varepsilon} d_t\right)\right) \quad (30)$$

where  $U_m$  is mean velocity below the trough level (offshore) given by the undertow.

Similarly, integrating from the trough level to the wave crest yields,

$$q_{sb} = \int_{d_t}^{d_c} U_b c_R \exp\left(-\frac{w_s}{\varepsilon} z\right) dz = \frac{U_b c_R \varepsilon}{w_s} 2 \sinh\left(\frac{H w_s}{2 \varepsilon}\right) \exp\left(-\frac{w_s h}{\varepsilon}\right) \quad (31)$$

where  $U_b$  is mean velocity above the trough level (onshore), derived from  $U_b = U_m d_t / H$  based on the continuity equation; the representative  $H$  is characterized by the rms wave height. Thus, the net transport due to suspended sediment transport (offshore) is given by  $q_{su} - q_{sb}$ .

### *2.3.4.2 Swash-zone transport*

The net swash-zone sediment transport rate over a cycle is calculated based on the formula derived by Larson et al. (2004b),

$$q_{bs} = K_c \frac{\tan \phi_m}{\tan^2 \phi_m - (dh/dx)^2} \frac{u_o^3}{g} \left( \frac{dh}{dx} - \tan \beta_e \right) \frac{t_o}{T} \quad (32)$$

where  $K_c$  is an empirical coefficient;  $\phi_m$  is the friction angle for a moving grain (about 30 deg);  $h$  is the local bed elevation of the foreshore;  $u_o$  is a scaling velocity;  $\beta_e$  is the local equilibrium slope (predicted by Kriebel et al. (1991));  $t_o$  is a scaling time;  $T$  is the swash period (assumed equal to the wave period).

The velocity variation in time at any location in the swash zone is assumed to be self-similar given by,

$$u / u_o = \Psi((t - t_s) / t_o) \quad (33)$$

where  $\Psi$  is an empirical function characterizing the shape of the temporal velocity variation;  $u_o$  is the wave front speed at uprush;  $t_s$  is the arrival time of the uprush at a particular location; and  $t_o$  is the duration of the swash at the particular location.

Based on ballistics model, the scaling velocity ( $u_o$ ) and time ( $t_o$ ) can be determined by,

$$\begin{aligned} u_o / u_s &= \sqrt{1 - h / R} \\ t_o / T &= \sqrt{1 - h / R} \end{aligned} \quad (34)$$

in which  $u_s$  is the wave front speed at the beginning of uprush; and  $R$  is the runup height (estimated by a Hunt-type runup formula).

In order to take into account some sediment diffusion between the swash and surf zone, an empirical expression is employed (Nam et al., 2009); where the additional sediment transport contributed by the swash zone is calculated through an exponential decay in the transport rate with distance from the seaward end of the swash zone. The additional transport rate is linearly added up to the sediment transport rate computed in the offshore and surf zone.

#### 2.3.4.3 Dune zone transport

According to the wave impact theory (Larson et al., 2004a; Overton et al., 1987), the weight of the sediment volume eroded from the dune is related to the force of the runup wave impacting the dune. The relationship can be expressed as,

$$\Delta W = C_E F \quad (35)$$

where  $C_E$  is an empirical coefficient;  $F$  is the swash force;  $\Delta W$  is the weight of the eroded volume given by,

$$\Delta W = \Delta V \rho_s (1 - p) g \quad (36)$$

in which  $\Delta V$  is the eroded volume;  $p$  is the porosity.

For a single bore, the swash force due to the change in the momentum of the bore hitting the dune can be estimated as,

$$F_o = \frac{d}{dt} (m_o u_o) = m_o \frac{du_o}{dt} \quad (37)$$

where  $m_o$  is the mass of the bore;  $u_o$  is the speed of the bore. According to Nishi and Kraus (1996), the mass of the bore is written as,

$$m_o = \frac{1}{2} \rho h_o s_o \quad (38)$$

in which  $h_o$  and  $s_o$  are the height and length of the bore, respectively. The deceleration of the bore is derived from,

$$\frac{du_o}{dt} \approx \frac{u_o}{T} \quad (39)$$

where  $T$  is the period at which waves hit the dune (taken to be equal to the incident wave period). According to Miller (1968), the speed of the bore is associated with the bore height expressed as,

$$u_o = C_u \sqrt{gh_o} \quad (40)$$

in which  $C_u$  is an empirical coefficient.

Substituting Eqs. (38) - (40) into Eq. (37) yields,

$$F_o = \frac{1}{2} \rho \frac{u_o^3}{gC_u^2} \frac{s_o}{T} \quad (41)$$

if the bore wavelength is assumed as the product between the bore speed and the period, the swash force for a single bore can be denoted as,

$$F_o = \frac{1}{2} \rho \frac{u_o^4}{gC_u^2} \quad (42)$$

regarding a number of bores impacting the dune in a period of time ( $\Delta t$ ), the total swash force may be written as,

$$F_o = \frac{1}{2} \rho \frac{u_o^4}{gC_u^2} \frac{\Delta t}{T} \quad (43)$$

where  $\Delta t/T$  represents the number of incoming waves.

Substituting Eqs. (43) and (36) into Eq. (35) and rearranging gives:

$$\frac{\Delta V}{\Delta t} = \frac{1}{2} \frac{C_E}{C_u^2} \frac{\rho}{\rho_s} \frac{u_o^4}{g^2 T} \frac{1}{(1-p)} \quad (44)$$

An average rate of dune erosion ( $q_D$ ) can be obtained,

$$q_D = \frac{dV}{dt} = -\frac{1}{2} \frac{C_E}{C_u^2} \frac{\rho}{\rho_s} \frac{u_o^4}{g^2 T} \frac{1}{(1-p)} \quad (45)$$

where a minus sign indicates that dune volume decreases with time.

Ignoring the effects of friction, the bore speed in front of the dune face, based on ballistics theory, can be estimated as,

$$u_o^2 = u_s^2 - 2gz_o \quad (46)$$

where  $z_o$  is the elevation difference between the dune foot and the beginning of the swash.

At the maximum of the runup ( $R$ ), the velocity  $u_o$  decreases to zero, where the wave front speed at the beginning of uprush is given by:

$$u_s^2 = 2gR \quad (47)$$

Substituting Eqs. (46) and (47) into Eq. (45) yields,

$$\frac{dV}{dt} = -4C_s \frac{(R - z_o)^2}{T} \quad (48)$$

where  $C_s$  is defined as,

$$C_s = \frac{1}{2} \frac{C_E}{C_u^2} \frac{\rho}{\rho_s} \frac{1}{(1-p)} \quad (49)$$

Assuming that  $R$  and  $z_o$  are constants, the following solution to Eq. (48) is obtained,

$$V = V_o - 4C_s (R - z_o)^2 \frac{t}{T} \quad (50)$$

where  $V_o$  is the initial volume of the dune. Thus, the eroded volume after time  $t$  may be derived from Eq. (50) to be,

$$\Delta V_E = V_o - V = 4C_s (R - z_o)^2 \frac{t}{T} \quad (51)$$

Eq. (51) is used to calculate the dune erosion at every time step. The eroded sediment from the dune is linearly distributed over the foreshore.

### 2.3.5 The effect of the long waves

In order to take into account the effect of long waves, a modified Hunt formula is developed, where the total runup height is determined by combining a probability density functions (pdf) for the runup height due to short waves based on the Hunt formula with a pdf describing the effect of the long waves on the water elevation at the shoreline.

For short waves, a Rayleigh pdf is assumed in the offshore leading to the following pdf for the runup height,

$$p_R(R) = \frac{4R^3}{R_{rms}^4} \exp\left(-\left(\frac{R}{R_{rms}}\right)^4\right) \quad (52)$$

where  $R_{rms}$  is obtained from the Hunt formula,

$$R_{rms} = \tan\beta \sqrt{H_{rmso} L_o} \quad (53)$$

where subscript  $o$  represents deep water conditions.

Integrating Eq. (52) and calculating the runup height ( $R_p$ ) corresponding to a certain exceedance probability yield:

$$R_p / R_{rms} = (\ln(1/p))^{1/4} \quad (54)$$

For long waves, the pdf is determined by a uniform distribution,

$$p_L(\eta_L) = \frac{1}{2a} \quad -a \leq \eta_L \leq a \quad (55)$$

where  $a$  is the amplitude. The pdf for the total runup height  $R_L = R + \eta_L$  is obtained by combining the pdfs in Eqs. (52) and (55) leading to:

$$\begin{aligned} p_{R_L}(R_L) &= 0 & R_L < -a \\ p_{R_L}(R_L) &= \frac{1}{2a} \left( 1 - \exp\left(-\frac{(R_L + a)^4}{R_{rms}^4}\right) \right) & -a \leq R_L \leq a \\ p_{R_L}(R_L) &= \frac{1}{2a} \left( \exp\left(-\frac{(R_L - a)^4}{R_{rms}^4}\right) - \exp\left(-\frac{(R_L + a)^4}{R_{rms}^4}\right) \right) & R_L > a \end{aligned} \quad (56)$$

In order to obtain the distribution function, integrating Eq. (56) yields,

$$\frac{R_{rms}}{8a} \left( \Gamma\left(\frac{1}{4}, \frac{(R_{Lp} - a)^4}{R_{rms}^4}\right) - \Gamma\left(\frac{1}{4}, \frac{(R_{Lp} + a)^4}{R_{rms}^4}\right) \right) = p \quad (57)$$

where  $R_{Lp}$  may be determined as a function of  $a/R_{rms}$  for different values of  $p$ ;  $\Gamma$  represents the incomplete gamma function.

Introducing non-dimensional quantities, Eq. (57) can be solved using a Newton-Raphson technique for  $R_{Lp}/R_{rms}$  as a function of  $a/R_{rms}$  for different values on  $p$ .

The relationship between the normalized long-wave amplitude ( $a/R_{rms}$ ) and the enhanced runup height ( $R_{Lp}/R_{rms}$ ) was derived in graphical form (see Figure 2) by numerically solving an equation based on a specific exceedance probability ( $p$ ). In

the beach profile change modeling, an exceedance probability of  $p = 0.02$  (2%) is typically selected as the representative runup height for calculating CS transport. Kriebel (1995) found for the SUPERTANK data that at the shoreline the low-frequency zero-moment wave height was more or less a constant ratio of the incident zero-moment wave height (about 0.3 to 0.4). Taken this to be valid for the rms wave height as well, and the amplitude to be half the wave height, the long-wave amplitude may be taken as approximately  $a = \delta H_{rmso}$ .

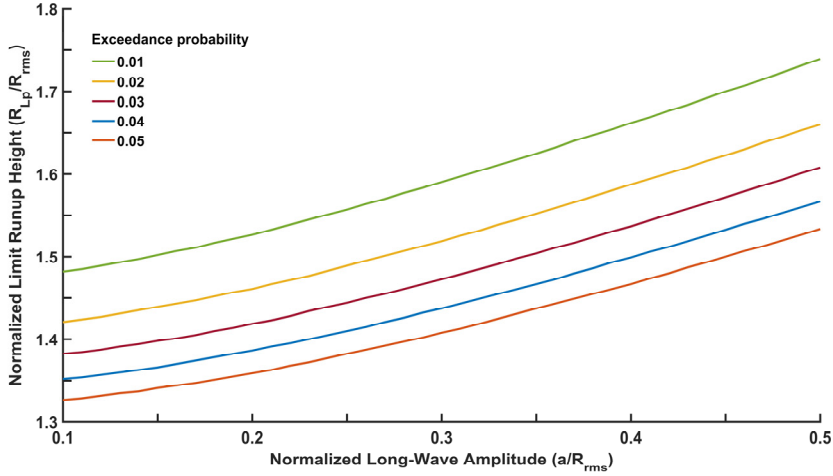


Figure 2. The relationship between the normalized long-wave amplitude ( $a/R_{rms}$ ) and the enhanced runup height ( $R_{Lp}/R_{rms}$ ) corresponding to a certain exceedance probability ( $p$ ).

The rms runup height is defined by:

$$R_{rms} = \tan \beta \sqrt{H_{rmso} L_o} \quad (58)$$

Taking the ratio between  $a$  and  $R_{rms}$  yields:

$$\frac{a}{R_{rms}} = \frac{\delta H_{rmso}}{\tan \beta \sqrt{H_{rmso} L_o}} = \frac{\delta}{\tan \beta} \sqrt{\frac{H_{rmso}}{L_o}} \quad (59)$$

Thus, this ratio can be expressed in terms of the deepwater wave steepness using the rms wave height. The value of  $\delta$  has to be specified (possibly used as a calibration parameter); based on the SUPERTANK data, it should be in the range 0.15-0.2. If a foreshore slope of  $\tan \beta = 0.1$  is used, then the multiplier before the square-root sign becomes around 2.0. Once the ratio  $a/R_{rms}$  is known, then the enhanced runup height ( $R_{Lp}/R_{rms}$ ) can be determined from the graphical solution.

However, the graphical solution has to be employed for every time step when applying this approach in the modeling for varying wave input.

In order to efficiently estimate the enhancement factor ( $= R_{Lp}/R_{rms}$ ), a faster approach to approximate the curve for exceedance probability 0.02 with an empirical function is proposed in this study. Using a third-order polynomial least-squares fitted to the exact solution yields:

$$\frac{R_{Lp}}{R_{rms}} = 1.401 + 0.0651 \frac{a}{R_{rms}} + 1.374 \left( \frac{a}{R_{rms}} \right)^2 - 0.940 \left( \frac{a}{R_{rms}} \right)^3 \quad (60)$$

The coefficient of determination for the fit is 0.99999 over the studied interval. Thus,  $a/R_{rms}$  can be calculated from the deepwater wave steepness following the equation above; then,  $R_{Lp}/R_{rms}$  is determined from the polynomial equation. The enhanced runup height,  $R_{Lp}$ , is used to compute the CS sediment transport in the swash zone and the dune region.

## 2.4 General insights into beach and dune evolution

As mentioned before, in this thesis study, the focus is mainly on sediment transport in the CS direction, assuming negligible longshore transport gradients. However, longshore sediment transport cannot be ignored in some cases, such as due to the shoreline orientation or interruption by structures. In addition, the impact mechanism of storms on the subaerial part of the beach profile in general cases is also of interest and should be clarified. Thus, general insights into the morphological behaviour of beach and dune driven by storms based on the work presented in **Paper IV** are given in this part, which is useful for model development and application.

### 2.4.1 Storm impact mechanism

Thirty-nine years of high-resolution data from 1981 to 2019 surveyed by the Field Research Facility (FRF) (Birkemeier and Forte, 2019) of the US Army Corps of Engineers at Duck, North Carolina, United States, were analyzed for temporal and spatial characteristics of beach morphology evolution, employing a range of statistical methods. In order to illustrate the varying behaviour during severe storms, three storms, including a subtropical cyclone (November 13-15 of 1981), an extratropical cyclone (February 23-25 and March 7-11 of 1989), and a tropical cyclone (October 28 to November 1 of 1991), and the associated profile responses, were analysed.

During the subtropical storm, the upper part of the berm and the lower part of the dune suffered severe erosion under the condition, in which the wave heights exceeded 3 m for 55 hours and the maximum water level was 1.51 m. For the second and third large storms, although the wave heights and water levels were high, minor

changes were observed in the dune region and accretion occurred in the upper part of the berm, which is because the waves could not reach the upper part of the dune face.

Thus, it can be concluded that dune erosion is jointly determined by water level and wave height and it could occur only when the total wave runup can attack the dune. The total wave runup can be roughly estimated by a simple measure of the runup height by using the deepwater wave height in combination with the water level. In addition, it was found that the dune portion of the FRF beach is quite stable and only rarely erodes if the combined water level and wave height is extreme. Thus, it was not suitable to select the FRF data as a field case for the model validation in the present thesis study.

#### 2.4.2 The effects of longshore transport

During the model development, it is assumed that gradients in the sediment transport are mainly in the CS direction. If waves approach and break towards the shoreline at an angle, longshore sediment transport (LST) is generated and if gradients occur in the LST, beach changes will result.

In order to investigate the importance of LST for the beach change, the LST rates were calculated based on a semi-empirical formula (USACE, 1984) using a time series of wave heights, periods, and incident angles from the FRF wave data. Sensitivity analysis corresponding to the mean yearly and monthly net LST rates for varying shoreline orientation were investigated. It showed that the net sediment transport is quite sensitive to the shoreline orientation, implying that accurate wave incident angle information is significant for sediment transport calculations.

In addition, structures on the beach, such as piers, groins, seawalls, as well as breakwaters can cause gradients in LST and result in beach change. In order to explore the morphological evolution of the subaerial region of the beach in terms of the influence of the FRF pier, the variation in the horizontal position with time for specific contours were investigated. The results displayed that the profiles south of the pier have experienced accretion, whereas the profiles north of the pier have exhibited long-term shoreline erosion, which is consistent with the general LST situation, that is, accretion occurs on the updrift side of the pier and erosion on the downdrift side.

Although the profiles selected were far away from the pier to minimize the influence of localized scour near the pier, the pier still had some influence on the beach morphology change. Thus, the LST cannot be ignored in beach profile change calculations, if there are some structures on the beach that induce LST gradients. In other words, for beaches with certain structures, the model developed in this thesis

study cannot be employed alone and routines for computing longshore transport have to be coupled to the current model.

# 3 Model application

*This chapter briefly presents the model applications for different cases. In section 3.1, the model is used to simulate beach profile evolution in the nearshore based on the work described in **Paper I**. In section 3.2, the model is applied to predict mound evolution in the offshore related to the work presented in **Paper II**. Finally, section 3.3 describes the model for simulating dune evolution corresponding to the work conducted in **Paper V**.*

## 3.1 Beach profile evolution in the nearshore

### 3.1.1 General description

Beach profile change during storms involves complex processes with strong interaction and coupling between waves, currents, sediment transport, and bed evolution. In general, high-energetic waves during storms often cause offshore transport and erosion, whereas low-energetic waves after storms induce onshore transport and accretion, which results in different beach behaviours, such as dune erosion, bar formation, berm flooding, and offshore mound evolution.

Quantifying the beach profile response is of great significance for coastal management. Extensive research has been dedicated to the beach profile response under varying waves and water levels, contributing to a number of empirical and theoretical equations and models. Most of the previous studies mainly focus on certain properties related to beach profile change. For example, at the earlier stage, whether a bar or berm would form and the geometric properties of bars and berms had arisen widespread concern. In subsequent model development, more attention was paid to dune erosion during storms, and less focus was put on bar formation.

However, the beach profile consists of different regions, including offshore, surf, swash, as well as dune zone, where different processes and transport relationships are employed. Thus, developing a numerical model that can simultaneously simulate the entire beach under varying waves and water levels is of importance. In this study, such a model is developed based on theoretical and empirical equations.

Although the equations employed in this model typically have been calibrated and validated for a range of cases, an important aspect of the model development is to ensure all model components are compatible. In addition, the effect of long waves is also considered to make the model more applicable for practical cases.

In order to test the performance of the model, different types of profile responses in the nearshore obtained from laboratory data are investigated in this section.

### 3.1.2 Data collection

The data used to calibrate and validate the model are obtained from the SUPERTANK laboratory data collection project (Kraus and Smith, 1994). In the SUPERTANK project, a 76-m-long beach with 104 m in length, 3.7 m in width, and 4.6 m in depth was constructed. The standard water level in the channel was 3.0 m and the input wave conditions were designed using predictive criteria described by Kraus et al. (1991). The sediment was uniform fine sand with median grain size diameter of 0.22 mm.

SUPERTANK ran for an 8-week period from 29 July to 20 September, 1991 and 20 major test cases were performed during the period. Four experimental cases encompassing three types of profile response, involving bar (ST\_10), berm (ST\_90), and offshore mound (ST\_J0, ST\_K0) evolution were chosen to calibrate and validate the model.

### 3.1.3 Model set up

During the simulations, the length of the computational domain, the grid spacing, and time step were 60 m, 0.5 m, and 60 s, respectively. The water level and  $d_{50}$  were 3.0 m and 0.22 mm, respectively. The input wave conditions, involving rms wave height, mean wave period, and duration of wave action for the experimental cases studied are tabulated in Table 1, where the rms wave height and mean period were recorded at the most seaward gage.

**Table 1. Input wave conditions for the experimental cases studied.**

Case	Rms wave height (m)	Mean wave period (s)	Duration (min)
ST_10	0.50-0.81	2.5-3.1	270
ST_90	0.48-0.53	2.4-2.5	50
ST_J0	0.45-0.46	2.4-2.5	150
ST_K0	0.46-0.47	2.5	220

As pointed out previously, the model contains of a number of modules; thus, some adjustments were still needed when the modules were put together to a complete model for simulating profile evolution. However, most of the empirical coefficients

in the theoretical formulas of different modules have been validated in earlier studies (Larson et al., 2015), which means limited need for recalibration. In this study, two coefficients concerning wave breaking and sediment transport were mainly tuned, whereas the other coefficients remained unchanged. The coefficient describing the contribution to sediment mixing by breaking waves was increased from 0.01 (employed by Camenen and Larson (2008)) to 0.15. Meanwhile, a constant multiplier of 7.0 was applied to Eq. (30) to achieve adequate transport related to undertow. In addition, a multiplier of 4.0 was employed in calculating the sediment transport rate due to wave asymmetry derived from Eq. (24).

The recalibration was conducted for case ST\_10 and the same parameters were then applied to the other experimental cases to validate the model. The details about the simulation results are presented in the following subsection.

### 3.1.4 Results

For all cases, the same calculated quantities, including the beach profile, rms wave height ( $H_{rms}$ ), and undertow velocity ( $U_m$ ) were compared with the SUPERTANK data as shown in Figures 3-6.

In Figure 3, the calculated profile reproduces the measured profile well in the subaerial part of the profile, whereas the calculated bar in the subaqueous profile is more subdued and located further offshore in comparison with the measured profile. However, the total bar volume is fairly similar between the calculations and measurements. The calculated wave height is in a good agreement with the measured wave height. Regarding the undertow velocity, the calculated velocity is underestimated compared to measured velocity, but their trends are consistent.

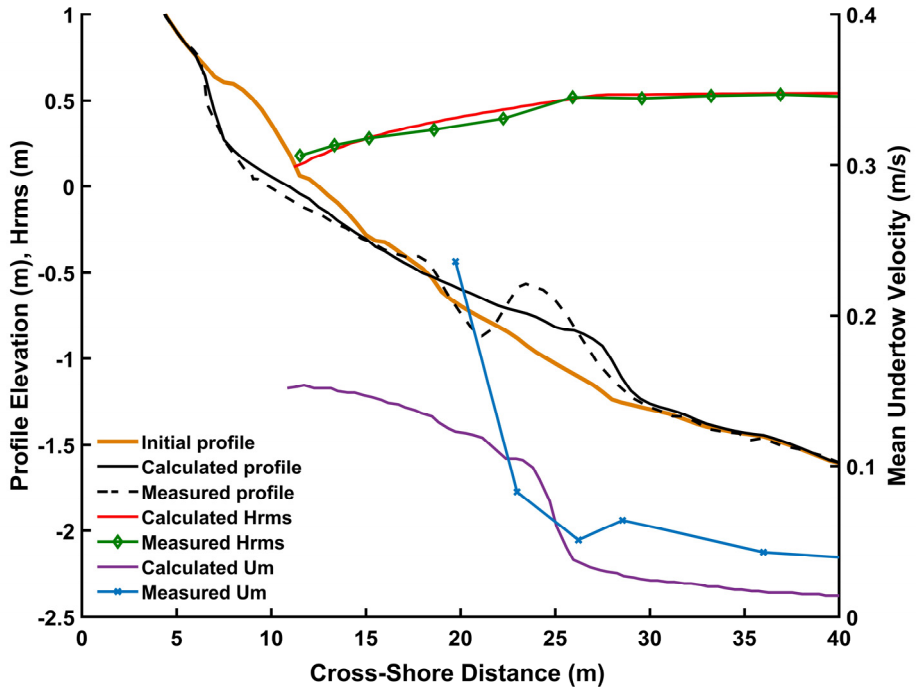


Figure 3. Calculated and measured beach profiles, wave height ( $H_{rms}$ ), and undertow velocity ( $U_m$ ) for case ST\_10 after 270 min of wave action.

Figure 4 shows that the berm is eroded rapidly and the sand is deposited around the still-water level. The calculated profile is well predicted except some parts of the profile. For instance, the most shoreward area is not reproduced well by the model, which indicates the model may not be able to calculate the sediment transport for a steep slope since the dune region has not been integrated into the model at the current stage. In addition, the seaward transport in the shoreline area is overestimated for the calculated profile. Regarding the wave height, it is well predicted except for the shallow water region. The calculated undertow is fairly constant compared to the measured undertow.

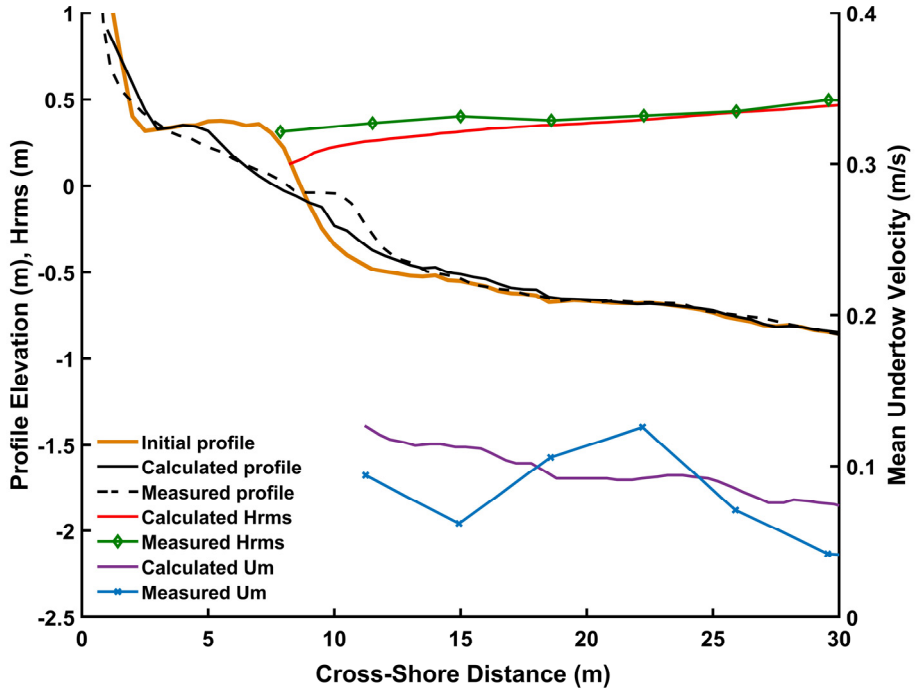


Figure 4. Calculated and measured beach profiles, wave height ( $H_{rms}$ ), and undertow velocity ( $U_m$ ) for case ST\_90 after 50 min of wave action.

In Figures 5 and 6, the calculated profiles with two types of offshore mounds, including a narrow-crested mound (ST\_J0) and a broad-crested (ST\_K0) mound, are in good agreement with measured profiles, respectively. For both mounds, a distinct trough in the mound evolves due to wave breaking and related energy dissipation on the mound, whereas the location of the calculated trough is more seaward compared to the measured mound. This may be because the wave transformation on the mound is nonlinear, whereas the employed wave model is not able to describe this phenomenon well. Since the mounds attenuate the incoming wave energy, and the inner part of the profile is rather close to its equilibrium shape, observed changes are small in this area, which the model is able to reproduce. The wave height is well predicted but the undertow velocity does not match very well.

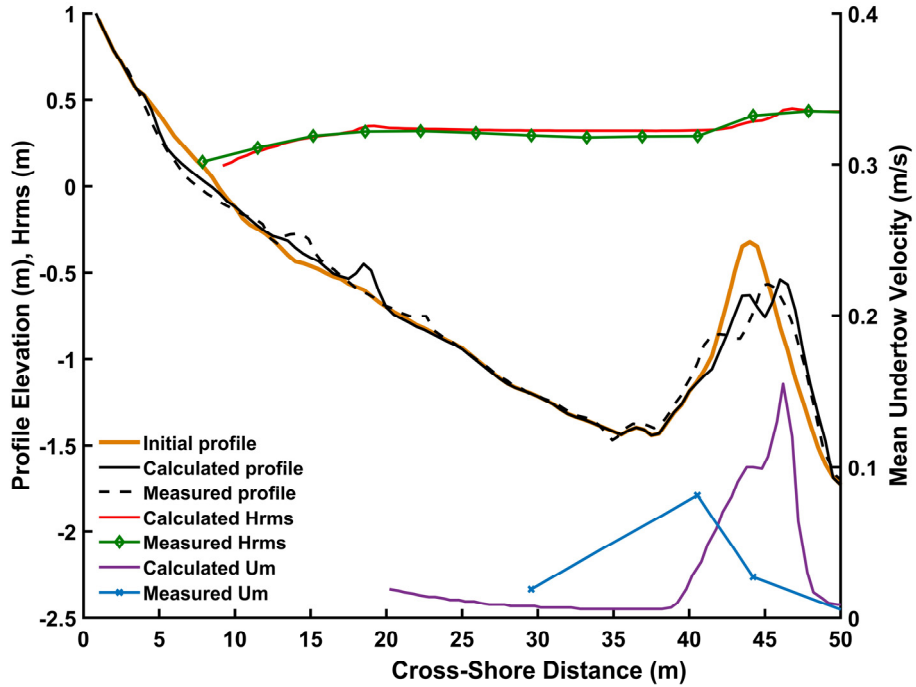


Figure 5. Calculated and measured beach profiles, wave height ( $H_{rms}$ ), and undertow velocity ( $U_m$ ) for case ST\_J0 after 150min of wave action.

In order to quantify model performance, the difference between the calculated and measured profiles is obtained by calculating the rms error (RMSE) and the Brier Skill Score (BSS) (Van Rijn et al., 2003).

The formulas are expressed as,

$$RMSE = \sqrt{\frac{\sum_{i=1}^n (y_{mi} - y_{ci})^2}{n}} \quad (61)$$

$$BSS = 1 - \left[ \left( \frac{\sum_{i=1}^n (|y_{ci} - y_{mi}| - \Delta y_m)^2}{n} \right) \right] / \left[ \left( \frac{\sum_{i=1}^n (y_{0i} - y_{mi})^2}{n} \right) \right] \quad (62)$$

where  $n$  is the number of values; subscripts  $m$  and  $c$  refer to measured and calculated respectively;  $\Delta y_m = 0.003$  m is the error in measured bed elevation in SUPERTANK (Kraus and Smith, 1994); and  $y_{0i}$  is the initial bed elevation.

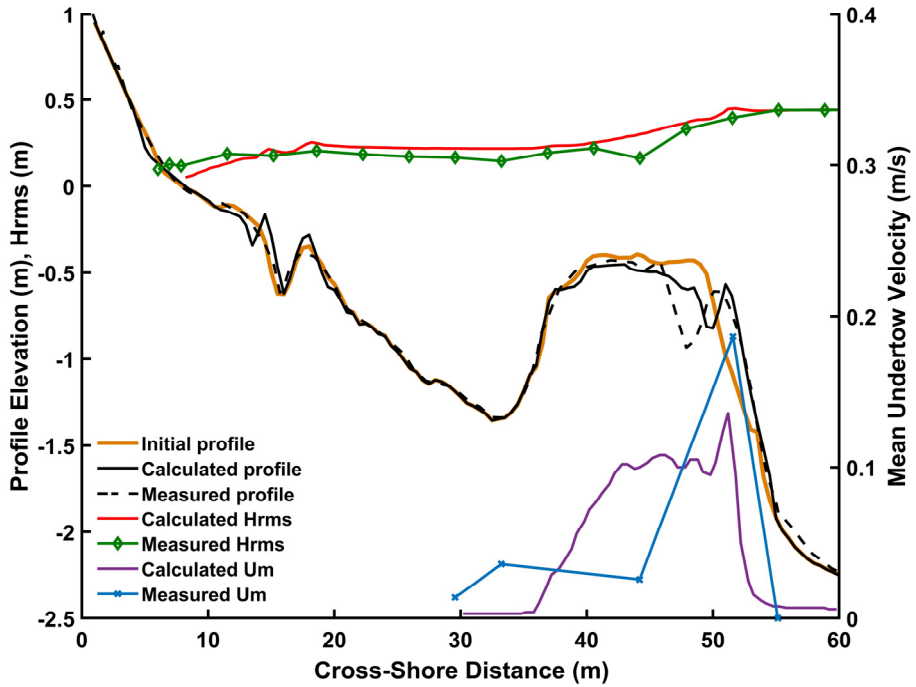


Figure 6. Calculated and measured beach profiles, wave height (Hrms), and undertow velocity (Um) for case ST\_K0 after 220min of wave action.

The RMSE and BSS of beach morphology for all cases were calculated and tabulated in Table 2. All values of RMSE are rather small which illustrates that the calculated profile is in good agreement with the measured profile for each case. In terms of BSS, all values are larger than 0.6 indicating that the model displays satisfactory performance denoted by “Good” according to Table 3.

Overall, the numerical model presents satisfactory skill in predicting beach morphology change.

Table 2. The RMSE and BSS of beach profile evolution for all cases.

Case	RMSE	BSS
ST_10	0.058	0.841
ST_90	0.044	0.779
ST_J0	0.062	0.689
ST_K0	0.073	0.622

**Table 3. The evaluation criteria of BSS for qualifying model performance.**

<b>BSS</b>	<b>Qualification</b>
1.0-0.8	Excellent
0.8-0.6	Good
0.6-0.3	Reasonable
0.3-0	Poor
<0	Bad

## 3.2 Mound evolution in the offshore

### 3.2.1 General description

Concerning shoreline retreat and beach erosion, beach nourishment has become the preferred remedy against coastal erosion in recent years. Nearshore mounds can dissipate wave energy and reduce the erosion on the shoreface. Simultaneously, wave breaking on the mounds contributes to the dispersion of sand onshore, leading to shoreface nourishment. Thus, a wide range of research on shoreface nourishment through the construction of offshore mounds have been conducted (Barnard et al., 2007; Larson and Hanson, 2015; Smith et al., 2017a; Smith et al., 2017b; Smith et al., 2015). However, it should be noted that the location of a nearshore mound is of importance in determining whether the mound is “active” or “stable” (Hall and Herron, 1950; Otay, 1994). For example, Van Rijn and Walstra (2004) found that the mound is stable for years in water depths between 10 m and 15 m, but active in water depths under 8 m. Therefore, to select the optimal design and placement of mounds, as well as to predict the evolution of the placed material, are challenges to coastal engineers and managers, but of great significance.

In this section, the above model, originally developed to simulate CS sediment transport and beach profile evolution in the nearshore, was used. However, the model was not rigorously tested and validated for transport in the offshore and the simulations were performed for limited periods of time when erosional conditions prevailed. Regarding mound evolution in the offshore over long time periods (several months or years), additional model development, such as equilibrium properties of the beach profile, is needed. In addition, since the mounds are constructed in the deep water, it is assumed that wave breaking is negligible and wave asymmetry dominates the transport.

Taking into account the effects of the local slope (Madsen, 1993; Madsen, 1991) in long-term simulation, the net Shields parameter in Eq. (21) can be modified as,

$$\theta_w^{net} = \frac{1}{4} \frac{f_w}{(s-1)gd_{50}} \left( u_c^2 \frac{T_c / T}{1 + \frac{\partial h / \partial x}{\tan \Phi_m}} - u_t^2 \frac{T_t / T}{1 - \frac{\partial h / \partial x}{\tan \Phi_m}} \right) \quad (63)$$

where  $\partial h / \partial x$  is the local slope ( $x$  is the cross-shore distance) and  $\Phi_m$  is the friction angle for a moving grain (taken to be 30 deg).

Substituting Eq. (22) into Eq. (63) yields,

$$\theta_w^{net} = \frac{1}{4} \frac{f_w}{(s-1)gd_{50}} \hat{u}^2 \left( \frac{\hat{q}_c}{1 + \frac{\partial h / \partial x}{\tan \Phi_m}} - \frac{\hat{q}_t}{1 - \frac{\partial h / \partial x}{\tan \Phi_m}} \right) \quad (64)$$

where the following definitions related to the onshore and offshore transport, respectively, were introduced:

$$\begin{aligned} \hat{q}_c &= \frac{u_c^2}{\hat{u}^2} \left( 1 - \frac{u_c}{\hat{u}} \right) \\ \hat{q}_t &= \frac{u_t^2}{\hat{u}^2} \left( 1 - \frac{u_t}{\hat{u}} \right) \end{aligned} \quad (65)$$

Multiplying the denominators within the brackets in Eq. (64) with their conjugate values and rearranging gives:

$$\theta_w^{net} = \frac{1}{4} \frac{f_w}{(s-1)gd_{50}} \frac{\hat{u}^2 \tan \Phi_m}{\tan^2 \Phi_m - (\partial h / \partial x)^2} \left( \hat{q}_c \left( \tan \Phi_m - \frac{\partial h}{\partial x} \right) - \hat{q}_t \left( \tan \Phi_m + \frac{\partial h}{\partial x} \right) \right) \quad (66)$$

At equilibrium conditions, the onshore and offshore transport balances each other, implying that  $\theta_w^{net} = 0$ , yielding,

$$\hat{q}_c \left( \tan \Phi_m - \frac{dh_e}{dx} \right) = \hat{q}_t \left( \tan \Phi_m + \frac{dh_e}{dx} \right) \quad (67)$$

in which subscript  $e$  denotes equilibrium conditions. Solving for the equilibrium slope gives:

$$\frac{dh_e}{dx} = \tan \Phi_m \left( \frac{\hat{q}_c - \hat{q}_t}{\hat{q}_c + \hat{q}_t} \right) \quad (68)$$

Substituting Eq. (68) into Eq. (66) leads to:

$$\theta_w^{net} = \frac{1}{4} \frac{f_w}{(s-1)gd_{50}} \frac{\hat{u}^2 \tan \Phi_m (\hat{q}_c + \hat{q}_t)}{\tan^2 \Phi_m - (\partial h / \partial x)^2} \left( \frac{dh_e}{dx} - \frac{\partial h}{\partial x} \right) \quad (69)$$

Substituting Eq. (69) into Eq. (18) yields,

$$q_b = a_w \frac{1}{2} \sqrt{\frac{f_w}{\tan \Phi_m}} d_{50} \hat{u} K_a^{1/2} \left| \frac{dh_e}{dx} - \frac{\partial h}{\partial x} \right|^{1/2} \text{sign} \left( \frac{dh_e}{dx} - \frac{\partial h}{\partial x} \right) \theta_{cw,m} \exp \left( -b \frac{\theta_{cr}}{\theta_{cw}} \right) \quad (70)$$

where the  $(\partial h / \partial x)^2$  can be neglected since it is typically much smaller than  $\tan^2 \Phi_m$ ; and  $K_a$  is given by,

$$K_a = \hat{q}_c + \hat{q}_t = \frac{u_c u_t}{\hat{u}^2} = \frac{u_c}{\hat{u}} \left( 1 - \frac{u_c}{\hat{u}} \right) \quad (71)$$

Similarly, using first-order cnoidal wave theory, it is found that  $K_a$  only varies with the Ursell number. Here, considering shallow water approximation, the Ursell number ( $U_r$ ) is defined as,

$$U_r = \frac{gHT^2}{h^2} \quad (72)$$

where wave period is used instead of wavelength in the previous formula displayed in **Chapter 2**.

For the same purpose of fast calculation of  $K_a$ , a set of polynomials using least-square fitting are obtained (details displayed in **Paper II**). Thus, Eq. (70) is employed to calculate the local transport at an offshore mound, where the equilibrium slope is estimated according to local surveys. Other coefficients remain at the default values based on previous studies.

### 3.2.2 Data collection

Data from the two field sites, Cocoa Beach and Perdido Key Beach in Florida, were used to calibrate and validate the model. Detailed information with regard to the field sites are given below.

#### 3.2.2.1 Cocoa Beach, Florida

Cocoa Beach is located south of Cape Canaveral Air Force Station spanning the Florida Department of Environmental Protection (FDEP) monuments from R26 to R40 (Hearin, 2014; Hearin, 2012), where a number of fill projects through constructing offshore mounds in water depths of 5.5-6.7 m have been widely conducted. In this study, the data regarding the mound response after the 1992 placement was collected and investigated. The offshore mound in 1992 was

constructed to be approximately 1.5 m in height, 100 m in width in the CS direction, and 915 m in the alongshore direction. The initial profile was selected from the central part of the mound, where the longshore transport was minimal and can be neglected. Two measured profiles after a time period of 136 days and 291 days after sand disposal were selected to calibrate and validate the model, respectively.

Wave data were available every 3 hr obtained from the Wave Information Study (WIS) at a water depth of 10 m and tidal data was given every 1 hr (Larson and Hanson, 2015). It should be recognized that the significant wave height collected from WIS was converted to rms wave height as the model input. The wave height  $H_{rms}$  varied between 0.16 and 2.98 m and the mean period between 3 and 18 s. The representative median grain size  $d_{50}$  was 0.15 mm.

#### 3.2.2.2 *Perdido Key Beach, Florida*

Perdido Key, located in Escambia County, Florida, is a narrow barrier island adjacent to Pensacola Pass to the east, Perdido Pass to the west, Gulf of Mexico to the south, and Big Lagoon to the north. In this site, the study area spanned from the Florida Department of Natural Resources (DNR) monuments Range 30 in the westernmost part to Range 67 in the easternmost part accompanied by 25 survey lines starting from a baseline with a 600 m spacing. The study area experienced severe erosion and the net erosion rate from 1974 to 1984 was about 1.5 m year<sup>-1</sup> according to Dean (1988). In order to counteract the erosion, a variety of beach nourishment projects have been carried out. In this study, a beach fill project conducted between 1989 and 1991 was selected. This project included two phases (Browder and Dean, 2000), shoreline placement and offshore mound placement, where the latter phase was studied here. The offshore mound was constructed to be 1.5 m in height, 300-800 m in width in the CS direction, and 3.5 km along the shoreline at a water depth of approximately 6 m in October 1991 (Work and Otay, 1997).

Two CS survey lines with two different initial mound shapes, one approximately in the central part of the mound and another at Range 58 (Work, 1990), were selected for modeling the sediment transport and profile response of the offshore mound. The representative median grain size  $d_{50}$  along these two survey lines were 0.33 mm and 0.31 mm, respectively, based on the grain size distributions for the sand samples discussed in Work (1990).

The wave data at a time step of 1 hour were collected from WIS at a water depth of 20 meters. The 20-min interval tidal elevations at the entrance of Pensacola Bay were generated using the model Wxtide32 version 4.7. The wave height  $H_{rms}$  varied between 0 and 2.02 m and the mean period between 2.43 and 10.15 s.

### 3.2.3 Model set up

Regarding Cocoa Beach, the length of the computational domain, the grid spacing, and time steps were 520 m, 10 m, and 20 min, respectively, where the wave and tidal data were interpolated to a time step of 20 min as well. Since no wave breaking occurred on the mounds, the sediment transport generated by wave breaking and undertow was ignored. Other parameter values from the model, as well as those emerging in the new transport formula, were kept at their standard values obtained in previous studies. The equilibrium profile was determined according to a theoretical Dean equilibrium profile which was derived by fitting it to the measured profile before the placement of the mound.

For Perdido Key Beach, the same grid spacing and time steps as for Cocoa Beach were used in this simulation and the wave data was also interpolated to 20 min. The equilibrium profile shape was estimated through a least-squares fitting between the Dean profile and the measured profile prior to mound placement. In addition, the same parameter values in the Coca Beach were employed for the Perdido Key validation.

### 3.2.4 Results

The comparison between the measurements and the simulations at a time period of 136 days after the sand disposal is shown in Figure 7 using default parameters (no special parameter tuning). The calculated profile displays a distinct spreading out of the placed sand, which is consistent with the measured profile, implying the model can predict the mound evolution well with default parameters. As mentioned above, the measured profile at a time period of 136 days was selected for model calibration, which may indicate the model can obtain a good enough result without parameter adjustment.

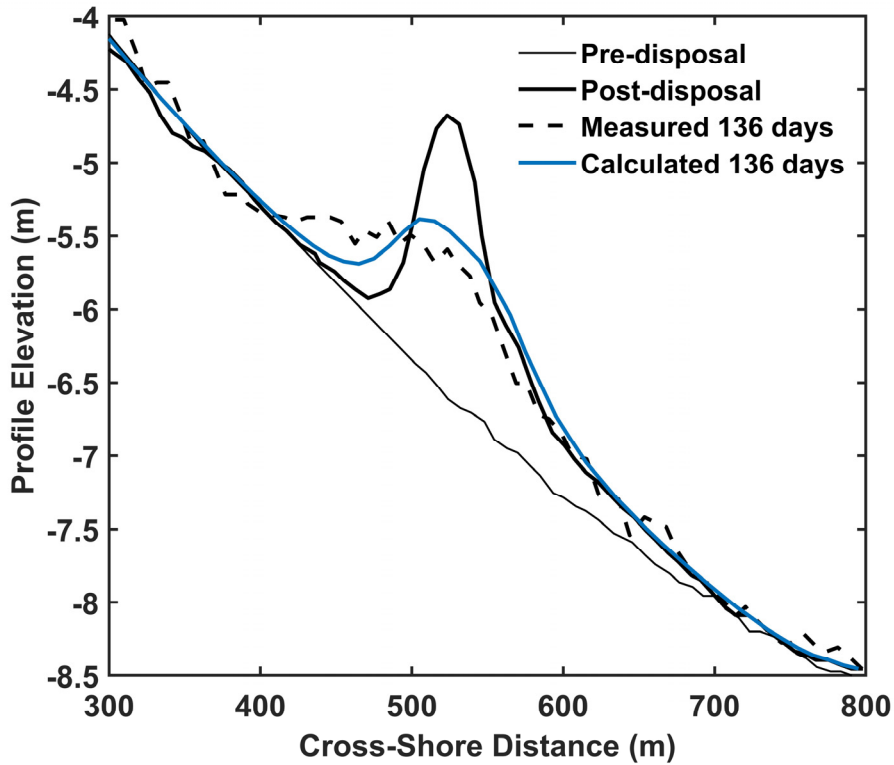


Figure 7. Comparisons between measured and calculated profiles 136 days after the sand disposal, Cocoa Beach.

In order to prove the conjecture, the mound evolution for a longer period (291 days) of wave exposure was investigated as shown in Figure 8. Obviously, most of the sand has been diffused away from the initial placement, resulting in a quite flat mound close to the equilibrium profile. It is interesting to note that the model simulation produced more satisfactory agreement for the mound evolution after 291 days in comparison with the evolution after 136 days, further indicating that the model can perform well enough with the default parameters. In spite of this, some attempts were still made to improve the agreement by applying a multiplier denoted as CTAS in Eq. (70) as discussed in the previous study. Four different CTAS values, from 1 to 4, were tested for the mound evolution after 136 days and 291 days, where CTAS=1 implies no change to the original Eq. (70). Although the calculated profile after 136 days agreed a bit better with the data if CTAS=2, the calculated profile after 291 days showed significantly poor agreement compared to CTAS=1. Thus, the original Eq. (70) without any modification to the transport parameters was used for subsequent simulations.

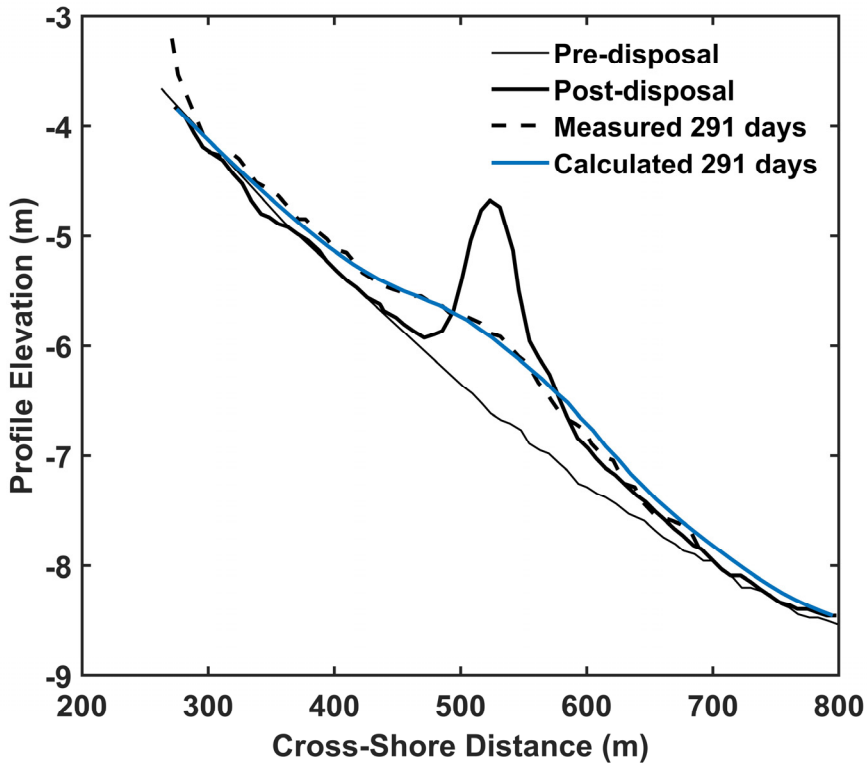


Figure 8. Comparisons between measured and calculated profiles 291 days after the sand disposal, Cocoa Beach.

From the above Figures 7 and 8, it is clearly seen that the mound diffuses away with time but the process of sediment transport across the mound is not clear. In order to explore this issue, the shape changes of the mound over time and the distribution of the total sediment transport across the profile at different times are depicted in Figures 9 and 10, respectively. Figure 9 shows that the mound spreads out faster with time at first and then diffuses more slowly when the profile is closer to equilibrium. Besides, more sand from the mound is transported onshore since the transport is larger in shallow water, which is beneficial from a perspective of nourishment.

In Figure 10, the positive values represent a direction of net transport towards the offshore and vice versa. It can be seen that the directions of net sediment transport rate on both sides of the dividing vertical line across the crest of the mound are opposite, which is consistent with the results in Figure 9. Generally, the total sediment transport rate gradually decays with time towards zero as equilibrium is

reached. However, the waves are varying constantly and the transport rate may be higher at specific times when the waves are large.

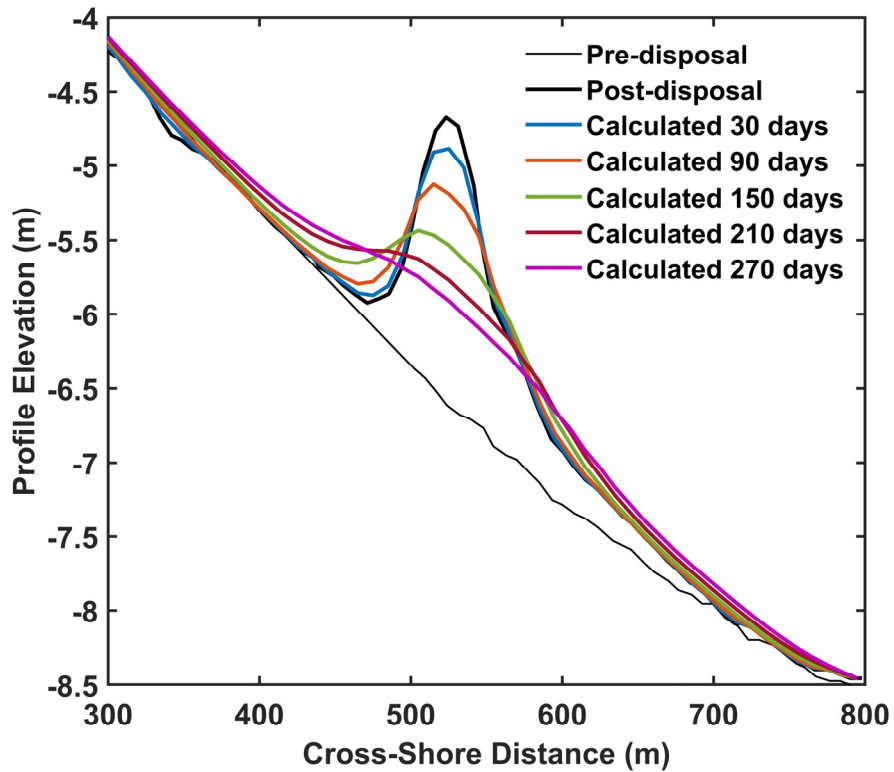


Figure 9. The evolution of the mound with time.

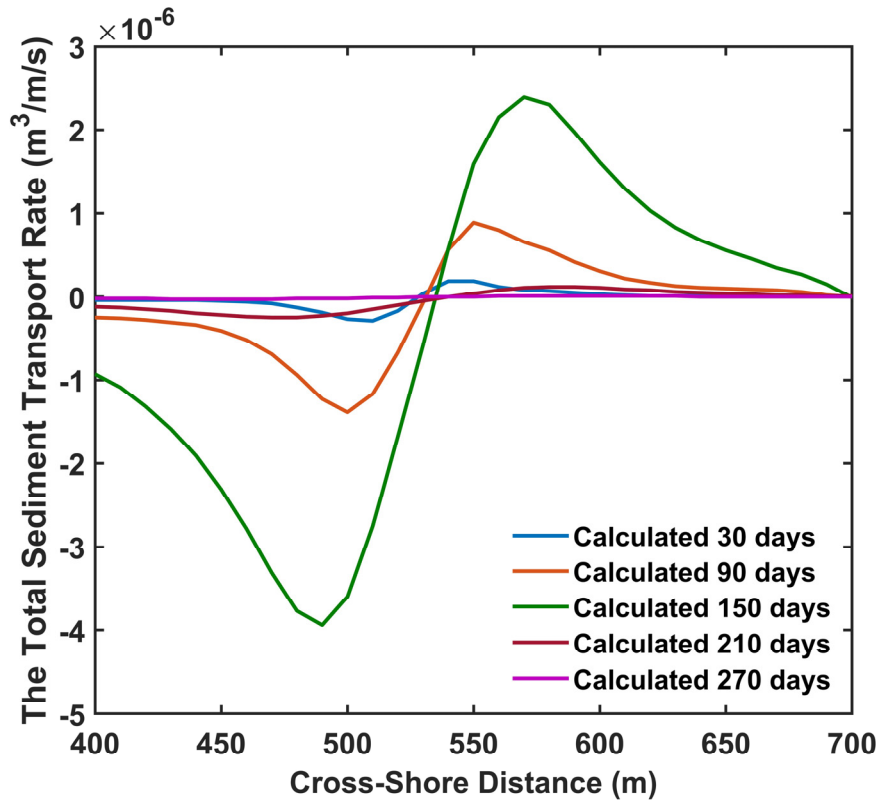


Figure 10. The distribution of the total sediment transport rate across the profile at different times.

Figure 11 and Figure 12 display the Perdido Key mound evolution with time at the midpoint of the mound and at Range 58 respectively. In both simulations, the calculated profile is in good agreement with the measured profile under one year of action by waves and tides. However, it is clearly seen that the spreading of the placed mounds in Perdido Key site is not as significant as in Coca Beach, which is not only owing to the different wave conditions at the two sites but also due to the initial shape of the mounds. The placed mound at Cocoa Beach is approximately a triangle and it is steep and narrow, whereas the mound at Perdido Key tends to a trapezoid and it is flat and wide. Thus, the sand diffusion rate is strongly influenced by the initial mound shape.

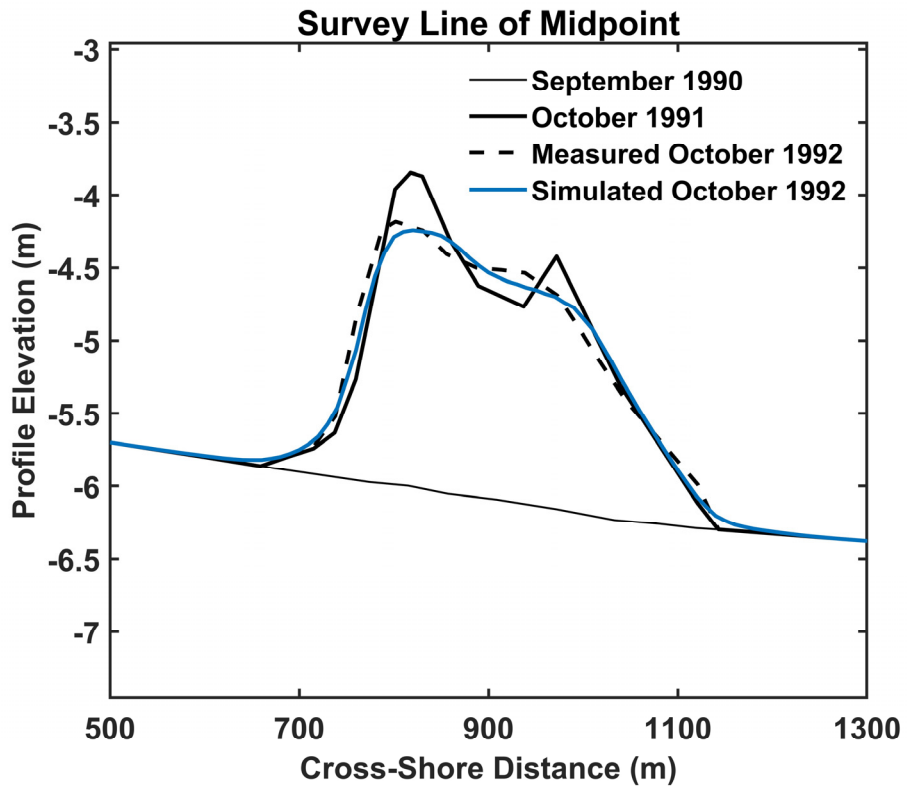


Figure 11. Calculated and measured profiles one year after mound placement at the midpoint of mound.

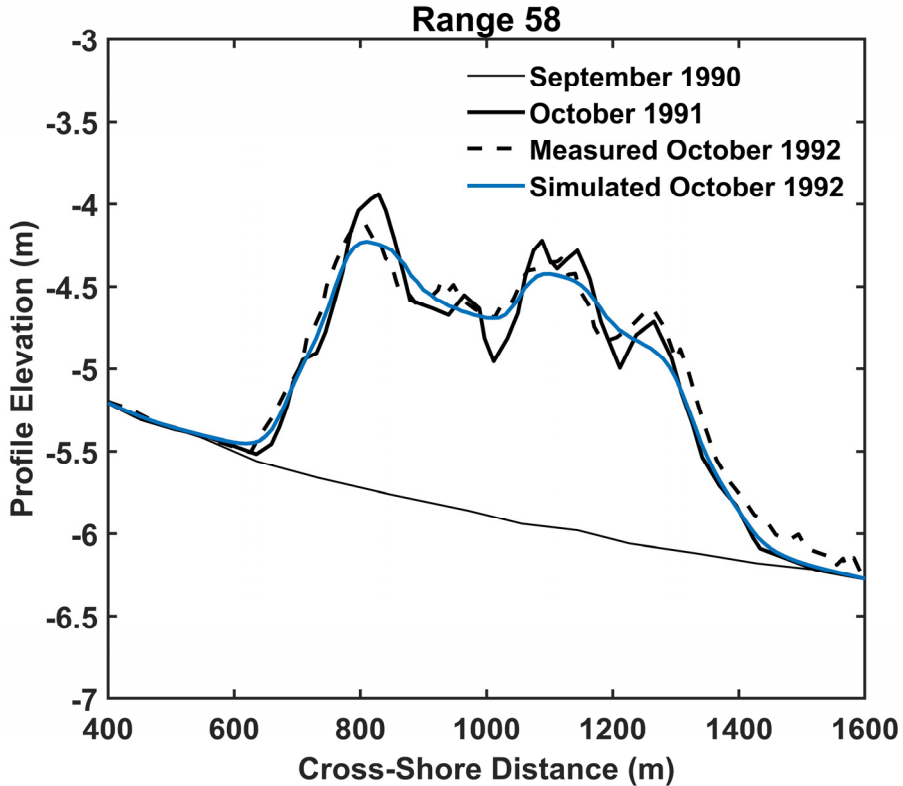


Figure 12. Calculated and measured profiles one year after mound placement for Range 58.

In order to explore the capability of the model to evaluate the effects of different mounds, two different scenarios with different mound volumes and locations were designed. A simple, triangular mound shape was selected, as an example, constructed based on the mound placed at Cocoa Beach, employing the general conditions there during the 291 days of simulation. The schematics of triangular mounds with different initial volumes and locations are shown in Figure 13 and Figure 14 respectively.

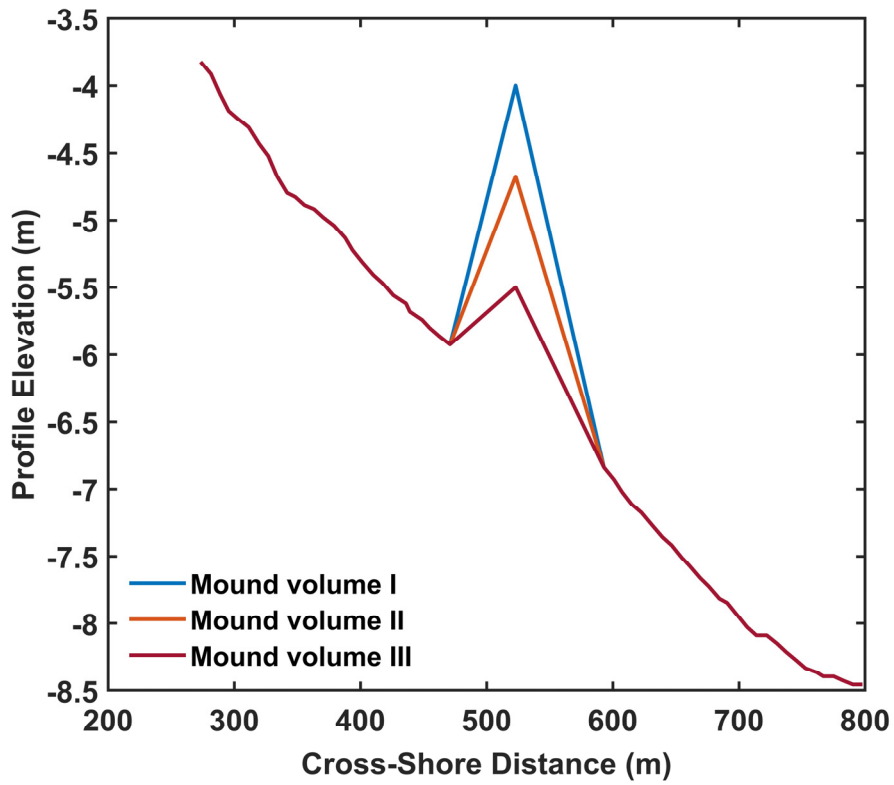


Figure 13. Schematic of triangular mounds with different initial volumes.

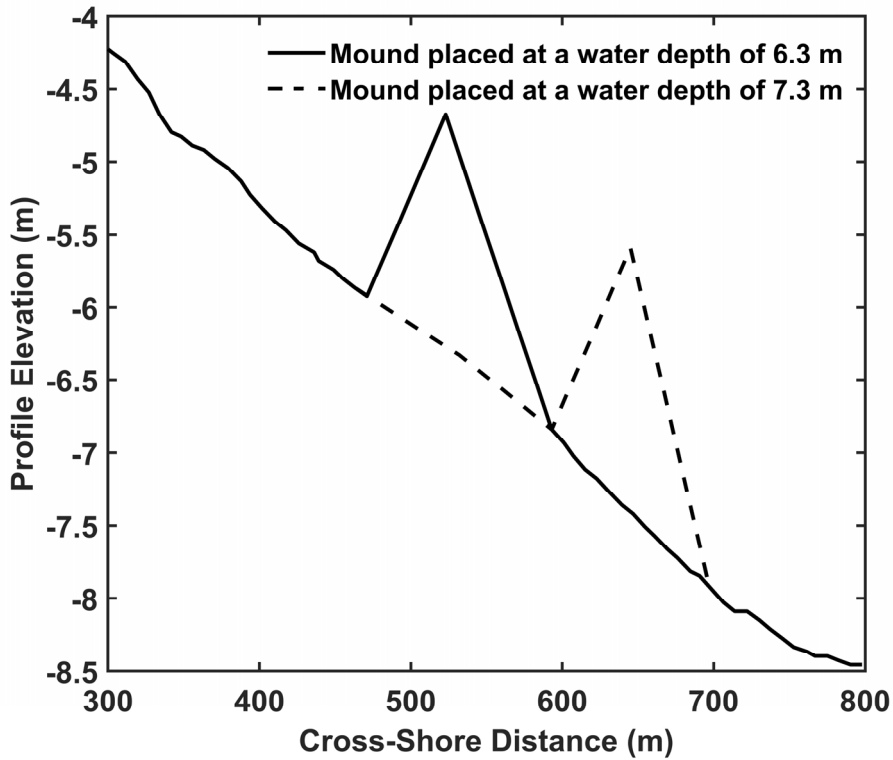


Figure 14. Schematic of triangular mounds placed at different water depths, but having the same initial volume.

In order to quantify the mound evolution with time for each scenario, the ratio ( $R$ ) between the remaining and initial mound volume at a specific time was calculated; the results are shown in Figure 15 and Figure 16.

Combining Figure 13 and Figure 15, it can be seen that the diffusion rate for all mounds with different initial volumes are increasing with time at the beginning and then decreasing to a small value, approaching a zero rate, illustrating that the mound diffuses fast at first and then slowly when the profile is closer to equilibrium. Besides, the ratio  $R$  changes the fastest for the smallest mound and the slowest for the largest mound, indicating that the smaller the mound, the higher the relative diffusion rate.

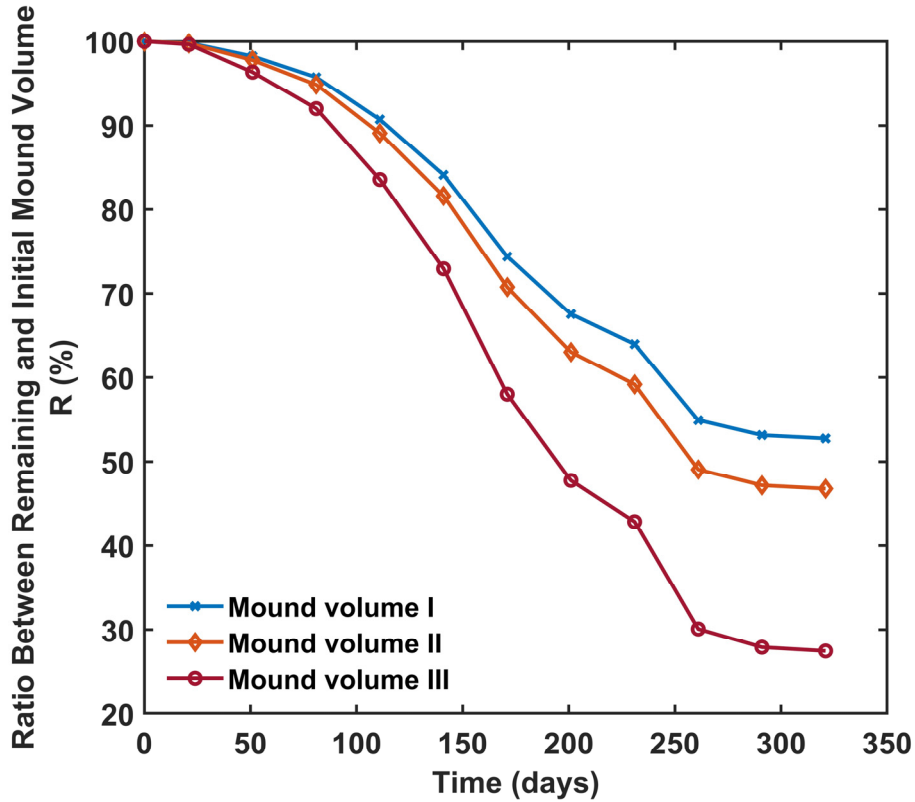


Figure 15. The ratio change between remaining and initial mound volume with time.

Viewing Figure 14 and Figure 16 together, it can be seen that the diffusion rates for both mounds increase at first and then decrease. However, the rate for the mound at a water depth of 7.3 m is slower than the mound at a water depth of 6.3 m, indicating the mound in deeper water is not as active as in shallower water from a transport perspective, which is consistent with previous studies. This simulation results can contribute to designing stable or active mounds based on the requirements given by coastal engineers and managers.

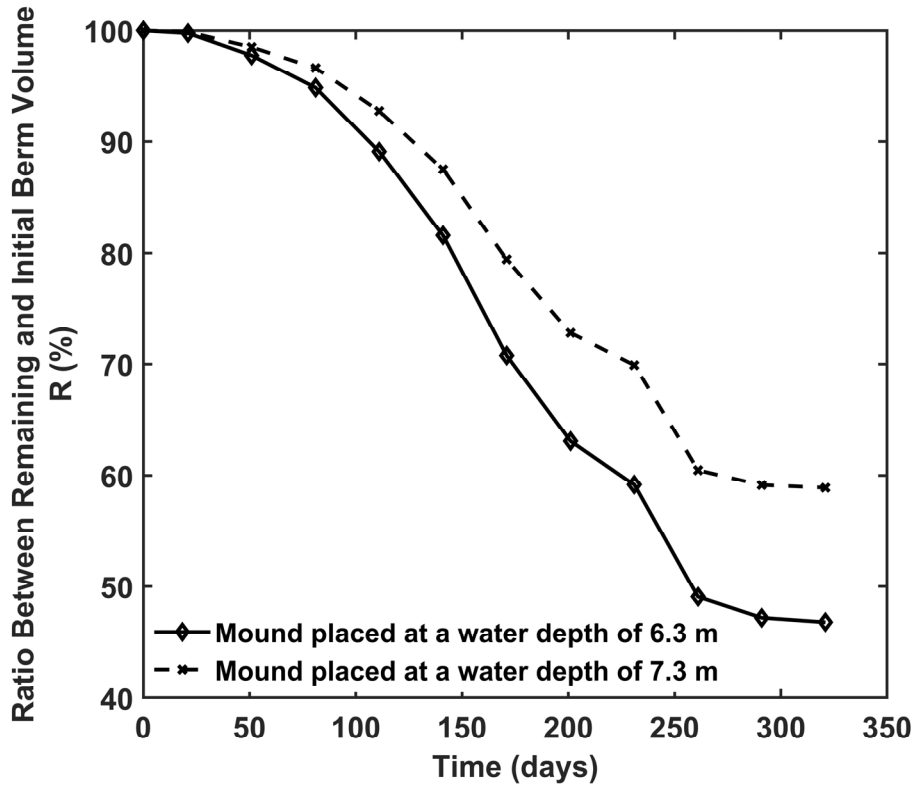


Figure 16. The ratio change between remaining and initial mound volume over time.

Overall, the numerical model is sufficiently reliable and robust in simulating a long-term offshore mound evolution in the deep water. Moreover, the model showed consistent behaviour with the previous studies in exploring the influence of mound design, which further demonstrates the capability of the model in simulating offshore mound evolution.

### 3.3 Dune evolution

#### 3.3.1 General description

Coastal dunes as parts of natural barriers are one of the most dynamic regions of the coastal area. They can not only provide important habitats for wildlife but also play a significant role in resisting storms. In general, coastal dunes can be divided into primary dunes (supply of sediment from the beach face), and secondary dunes

(supply of sediment from primary dunes) (Sloss, 2012). It should be noted that the dunes investigated in this study refer to primary dunes (foredunes). On many beaches, the dunes constitute the last defense against flooding and erosion. Once the dunes are overtopped or breached, it may lead to serious damage to the infrastructure and property in the coastal area. In addition, due to climate change, sea levels are expected to rise and stronger storms are projected to increase, resulting in dune inundation, which threatens the integrity of the dunes and further aggravates the vulnerability of the coastal system. Thus, quantitatively understanding the dune erosion processes driven by storms is of significance for coastal safety and sustainable development.

A variety of process-based models, including numerical models (Armaroli et al., 2013; Dissanayake et al., 2014; Dissanayake et al., 2015; Harley and Ciavola, 2013; Johnson et al., 2012; Larson and Kraus, 1989; Lindemer et al., 2010; McCall et al., 2010; Roelvink et al., 2009; van Rijn, 2009; Williams et al., 2011) and empirical models (Erikson et al., 2007; Kobayashi, 1987; Larson et al., 2004a; Palmsten and Holman, 2012) for predicting the dune evolution have been developed.

In general, numerical models for predicting the evolution of the dune profile during storms can be divided into two approaches, including the equilibrium profile and the wave impact theory. The former approach hypothesizes dune retreat through avalanching algorithm, that is, the dune collapses when the dune slope exceeds an equilibrium slope (Larson and Kraus, 1989; Roelvink et al., 2009). The latter approach assumes dune erosion is related to the wave impact, that is, the sediment volume eroded from the dune is proportional to the force of the waves hitting the dune (Larson et al., 2004a; Overton et al., 1994). Compared to the avalanching algorithm that geometrically determines the dune erosion, the wave impact theory is a more physically based approach in estimating the sediment transport, although it still relies on empirical observations.

Although the above models are applicable for predicting dune evolution, most of them only focus on the dune region rather than the entire beach. It should be noted that the dunes are integral parts of the subaerial beach where the morphology of the dunes is dependent on the sand exchange between the dune and the beach, which means that the evolution of the dunes should be investigated in conjunction with the response of the other parts of the beach.

Thus, in this section, the dune module is developed to obtain a complete numerical model to simulate beach and dune evolution during storms.

### 3.3.2 Data collection

Here, two types of cases, including laboratory cases and field cases were compiled for model calibration and validation. The general description of different cases,

including the overview of the study area, wave conditions, and water levels, are described below.

### 3.3.2.1 *Laboratory Data*

The laboratory cases were also selected from the SUPERTANK laboratory data collection project. In this study, two experimental cases, including ST\_50 and ST\_60, related to dune erosion were chosen.

### 3.3.2.2 *Field Data*

The field cases selected for this study includes two cases from Ocean City, Maryland and one case from Myrtle Beach, South Carolina. Ocean City is a major beach resort area in Worcester County, Maryland, United States (Wise et al., 1996). During the period from October 1991 to January 1992, a series of storms, including the Halloween storm (30 October 1991), 11 November 1991 storm, and 4 January 1992 storm occurred. These storms caused severe erosion on the beach and dune, which provide suitable data for evaluating the model. Two different beach profiles, along survey lines 81 and 45 (Wise et al., 1996) were selected for model testing. The surveys before and after the studied period for profile 81 was impacted by all the above three storms (case OJ81) from October 1991 to January 1992, whereas corresponding surveys for profile 45 was only impacted by the Halloween storm (case HAL45). A median sediment grain size 0.35 mm was selected for all beach profiles in Ocean City.

Myrtle Beach is a coastal city located in Horry County, South Carolina, United States. Around midnight September 22, 1989, Hurricane Hugo made landfall north of Charleston, SC. Hurricane Hugo produced tremendous storm surge along the coast and caused severe erosion on Myrtle Beach. A single profile line of Myrtle Beach is available for modelling beach and dune response to Hurricane Hugo in the present study. The median sediment grain size in this site is 0.20 mm.

### 3.3.3 *Model set up*

The input conditions, including root-mean-square (rms) wave height ( $H_{rms}$ ), mean wave period, and water level for all above cases studied in this paper are given in Table 4. The incident wave angle is not included, assuming that the waves are close to perpendicular to shore at the input location. In this study, ST\_50 was used to calibrate the model and the other cases were used to validate the model.

**Table 4. Input wave conditions for all cases studied.**

Case	Rms wave height (m)	Mean wave period (s)	Water level (m)
ST_50	0.33 - 0.54	2.4 - 3.7	-0.15 - 0.15
ST_60	0.31 - 0.50	2.5 - 3.5	0.15 - 0.30
OJ81	0.34 - 2.93	4.7 - 19.7	-0.5 - 2.0
HAL45	0.44 - 2.19	6.9 - 19.7	-0.5 - 1.6
Myrtle Beach	0.14 - 3.10	7 - 14	-0.43 - 2.32

There are two parameters, wave runup height ( $R$ ) and the empirical dune transport coefficient ( $C_s$ ), that should first be considered since these two parameters are critical in determining the amount of dune erosion as shown in Eq. (51). Regarding the wave runup height, the enhancement factor for the runup due to long waves was calculated at every time step based on the simple approach for varying input wave conditions. With respect to the  $C_s$  value, its range has been investigated by Larson et al. (2004a). In this study,  $C_s=0.16\times10^{-3}$  was chosen and applied in all simulation cases.

In addition, another two coefficients, one related to bed load due to wave asymmetry and one related to suspended load below trough, were recalibrated. Although these two coefficients had been tuned in the previous study, some adjustments were deemed necessary when the model is employed to more general conditions, such as field cases. In this study, the former coefficient was changed from 4 to 1, and the latter coefficient was changed from 7 to 3. All other coefficients were kept at their default values from the previous studies.

### 3.3.4 Results

Figure 17 shows the comparison between the measurements and the simulation results for ST\_50 after 120 and 180 minutes of wave action, respectively. The calculated profiles are in good agreement with the measured data in both the dune region and beach region. In Figure 17, it is clearly seen that the dune face keeps retreating shoreward with time since the runup waves can reach the dune and attack it at all times.

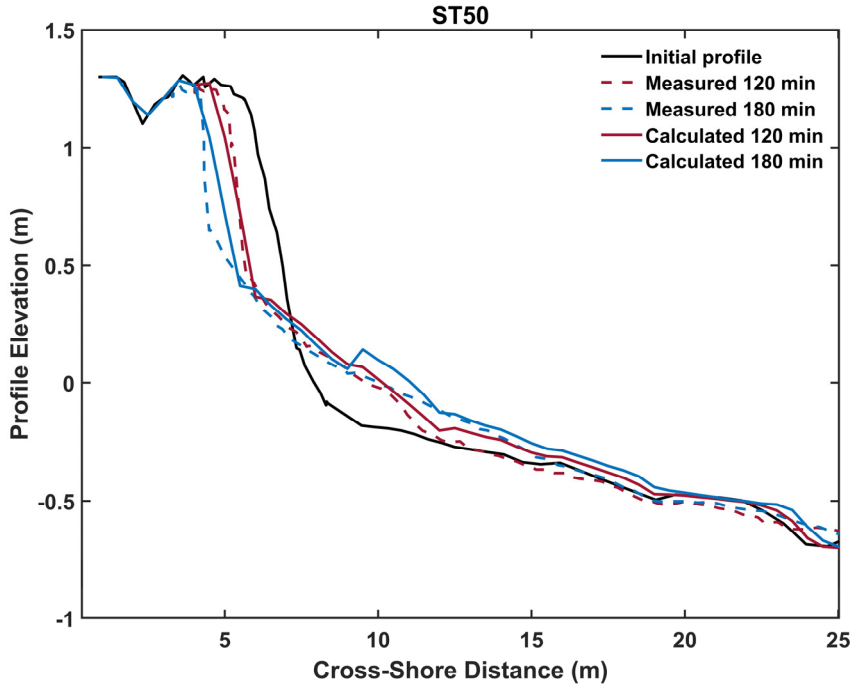


Figure 17. Calculated and measured beach profiles for Case ST\_50 after 120 min and 180 min of wave action, respectively.

The calculated and measured profiles for ST\_60 after 80 and 160 minutes of wave action are displayed in Figure 18, respectively. The figure shows that the dune is constantly eroding with time under the wave attack. The dune face after 80 minutes of wave action is well reproduced in comparison with the measured profile, whereas the amount of sand deposited in the swash zone is overpredicted. Regarding the computed profile after 160 minutes of wave action, the dune face recession is underestimated while the shape of the dune is well captured. Similarly, the sand volume in the swash zone after 160 minutes is also overestimated. The main reason for the overestimation of the sand volume in the swash zone is that the water level is high (up to 0.3 m) corresponding to a shorter distance between the dune toe and the shoreline, implying more sand is distributed in this region. It indicates that the linear algorithm in the model for distributing the eroded sand from the dune to the swash zone may need to be further improved, if the water level is rather high with regard to the dune toe.

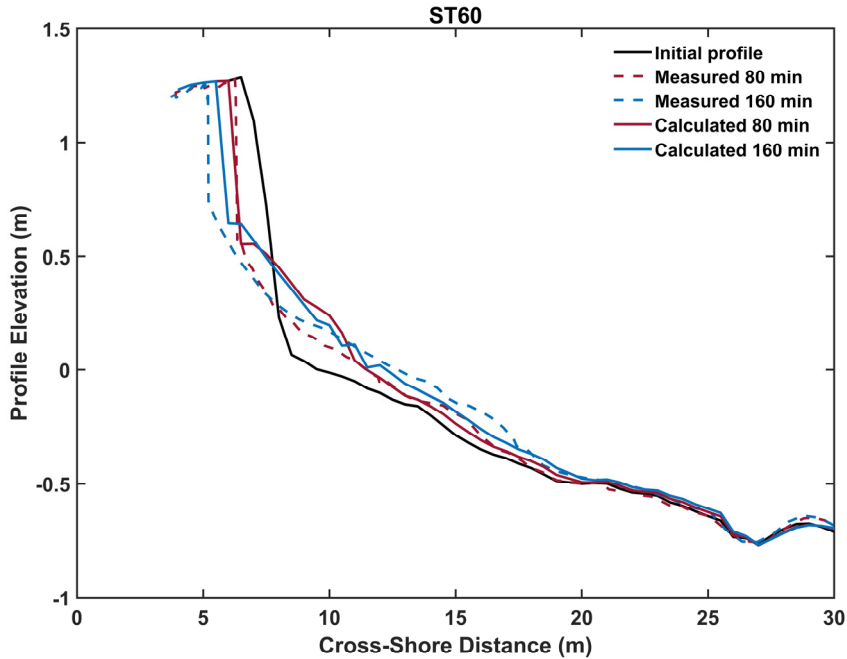


Figure 18. Calculated and measured beach profiles for Case ST\_60 after 80 min and 160 min of wave action, respectively.

Figure 19 shows a comparison of the simulation and measurement results of profile 81 under the OJ storm series in Ocean City, MD. As shown in Figure 19(a), the simulated profile matches well the observed profile, except for the local shape of certain morphological features, after the series of storms hit during the period from October 1991 to January 1992. For example, the model simulation produces poor agreement in the foreshore, where a post-storm berm due to beach recovery under low-energy waves appears in the upper part of the measured profile, as clearly shown in Figure 19(b). It indicates that the model cannot capture post-storm accretion, which is a weakness of the model that should be improved in the future. In addition, a portion of sand in the upper part of the dune crest is eroded, as displayed in the measured profile, whereas it is not reproduced by the model. This may be because of overwash; no such algorithm is included in the model at present.

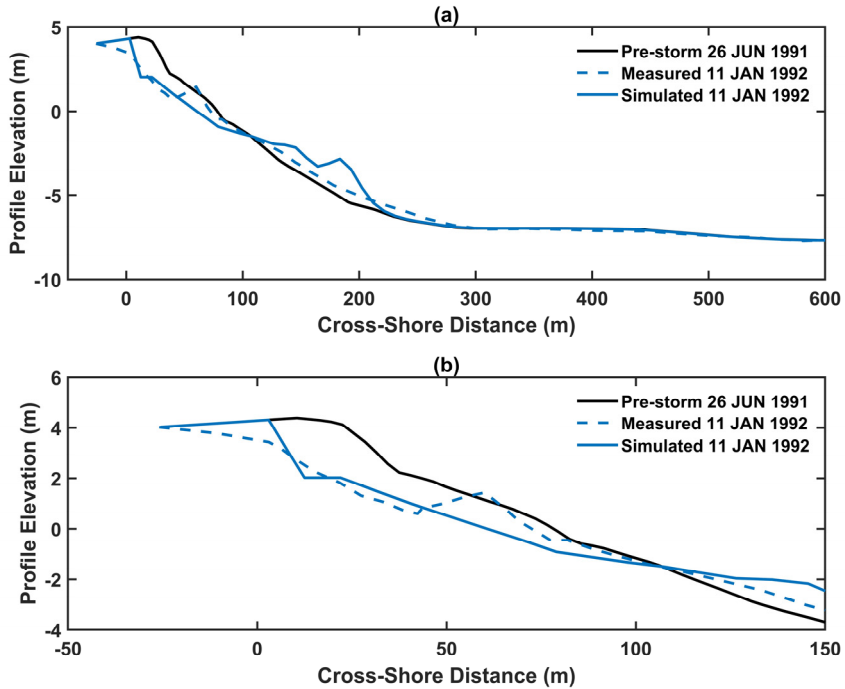


Figure 19. Calculated and measured beach profiles of the OJ storm series for profile 81, Ocean City, MD: (a) the entire beach profile; (b) the upper part of the beach profile.

Figure 20 displays the comparison between the measurements and the simulation results for profile 45 under the Halloween storm. Although the amount of foreshore erosion is underestimated compared to the measured profile, the evolution of dune region agreed rather well. In this figure, the simulated bar is more offshore in comparison with the measured bar. Although the calculated bar is not predicted well, the total bar volume is quite similar in the measurements and simulations.

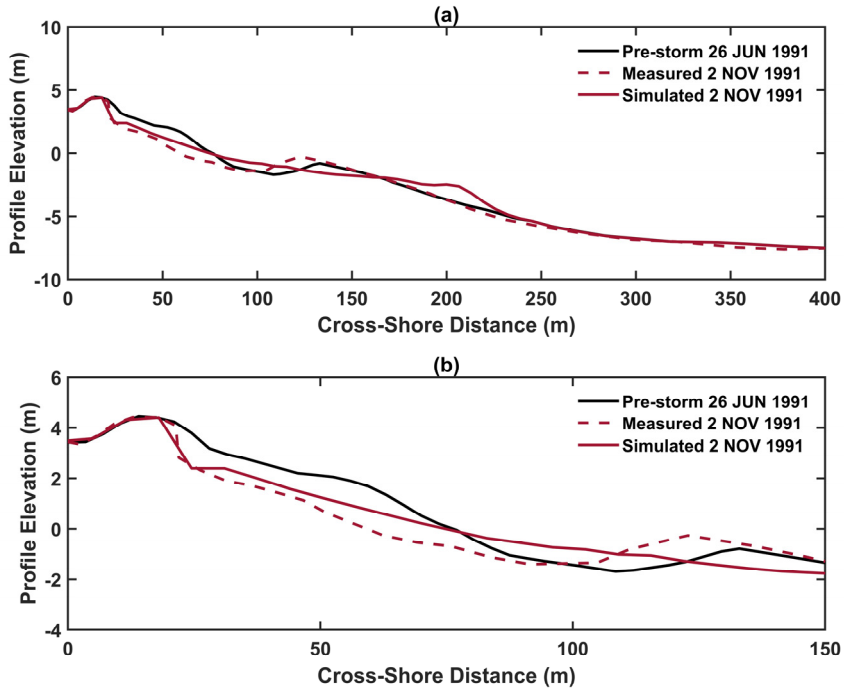


Figure 20. Calculated and measured beach profiles of the Halloween storm for profile 45, Ocean City, MD: (a) the entire beach profile; (b) the upper part of the beach profile.

Figure 21 shows the simulations and measurement results for Myrtle Beach after Hurricane Hugo. The amount of sand erosion is underestimated in the dune region, which may also be due to overwash (no algorithm included); overwash implies a portion of the waves passing over the dune and washing sand onshore. In addition, although the amount of sand erosion is overestimated on the foreshore and in the shallow water regions, the shape of the measured profile is predicted rather well in the calculations.

Overall, the new model to simulate beach and dune response seems to reliably capture the main governing processes and general morphological behaviour, which has great potential in practical engineering projects.

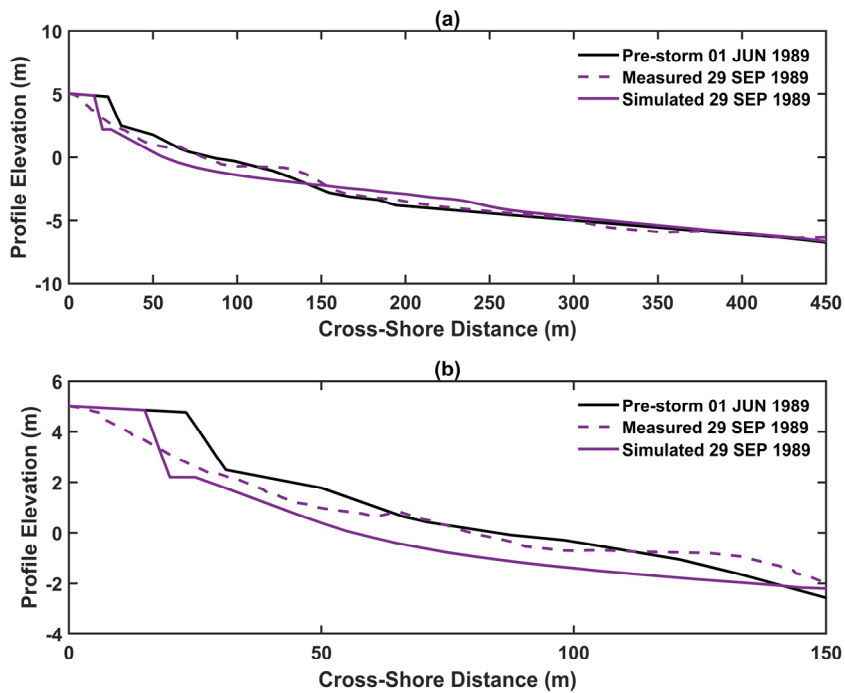


Figure 21. Calculated and measured beach profiles of the Hurricane Hugo for Myrtle Beach, SC: (a) the entire beach profile; (b) the upper part of the beach profile.

# 4 Discussion

*In this chapter, the novelty of the present model in comparison with previous applications of the different model components, as well as compared to other existing models, is first reviewed. Then the model limitations and future improvements are discussed.*

## 4.1 Model novelty

Sediment transport during storms and associated changes in the beach and dune profile takes place in a very energetic and complex environment. Large quantities of sand from the beach and the dunes are typically transported offshore, threatening the integrity of the beach and the dunes, which may result in loss of properties and possibly lives. The capability to quantify storm erosion is becoming increasingly important in coastal management and protection.

Early studies were dedicated to understanding the processes and formulating empirical equations based on laboratory investigations or field analysis. Accompanying a deeper understanding of the physical mechanisms of beach and dune profile evolution, a variety of numerical models have rapidly evolved. Although these models could predict the beach profile evolution through embedding physical processes, most of them often lack robust and reliable descriptions of all relevant processes throughout the regions of the profile, especially in the subaerial region that includes the foreshore, berm, and dune.

In this thesis work, a new numerical model was proposed that can simulate the beach and dune evolution employing physics-based equations at an appropriate level for simulations in engineering studies. A variety of modules, including wave transformation, CS currents, CS sediment transport, which were developed and validated in previous studies with substantial amounts of data, were put together for the first time and further developed. Some key parameters, including coefficients related to bed and suspended load transport and dune erosion, were recalibrated to achieve optimum agreement with observed beach profile evolution.

In order to consider the influence of long waves, an enhancement factor to the runup height was proposed, which is a completely new method. Moreover, instead of

deriving the enhancement factor from the graphical solution, a simple and faster method was developed for varying wave input.

In addition, the transport due to seaward diffusion of sediment from the swash zone to the surf zone and the distribution of eroded sand from the dune to the swash zone contain novel elements as well.

Moreover, the model is sufficiently reliable and robust when it was applied to simulate the evolution of offshore mounds. The model also proved to be a useful tool in selecting the optimal design and placement of mounds that is of great significance for coastal engineers and managers.

Overall, the model, containing a number of components to simulate the main governing processes along the beach and dune, is reliable and robust, implying that it can be a new, useful approach to simulate CS sediment transport and beach profile change.

## 4.2 Model limitations and future improvements

This study proposed a new model to simulate the CS sediment transport and beach profile response under varying waves and water levels. Although the model displays quantitative skill in predicting beach and dune morphology change, some limitations are worth noting. For example, possible longshore gradients that can cause changes in the profile shape are ignored. However, longshore sediment transport is a common process occurring on exposed beaches due to changes in shoreline orientation or interruption by structures.

Besides, overwash is not yet integrated into the model when considering the impact of waves on the dune. According to Sallenger Jr (2000), the impact of waves on the dune can be divided into four regimes, including swash, collision, overwash, and inundation. In terms of swash and collision, the model can describe the behaviour of the dune. The inundation regime means that the entire dune is inundated by water; in effect, the dune is more or less located in the surf zone, which might be simulated by the model. However, for the overwash regime, as runup overtops the dune, water can flow landward, leading to dune erosion and sand deposition landward of the crest, which requires a different algorithm not implemented in the present model, but could be included in subsequent model development.

In addition, the model cannot well reproduce the post-storm recovery in the swash zone. Although the model involves the main mechanisms for onshore transport and accretion in the swash zone, other factors should be considered, related to the wave transformation when a limited surf zone appears. In the next step, the model will

focus on improving the capability to simulate onshore transport and accretion in the nearshore.

Furthermore, the model is primarily suitable for simulating the beach and dune evolution on the time scale of storms, although simulations were performed for longer-term evolution of offshore mounds. However, regarding time scales from years to decades, additional efforts should be made to develop and validate the model.

## 5 Conclusions

In this thesis work, a numerical model for simulating beach and dune evolution due to varying waves and water levels was developed. A variety of modules, including wave transformation, CS currents, mean water elevation, CS sediment transport, and profile evolution, were integrated into a model including relevant physics in combination with empirical information. The model was applied to different types of beach profile response, including nearshore profile evolution (section 3.1), offshore mound evolution (section 3.2), and dune erosion (section 3.3).

In the first application, three types of cases involving bar, berm, and offshore mound, were investigated employing laboratory data obtained from the SUPERTANK laboratory data collection project. Calculated hydrodynamic quantities, involving the rms wave height, undertow velocity, and beach profile evolution were compared with measured data. The rms wave height showed good agreement between measurements and calculations, whereas the undertow results showed less agreement. Regarding the profile evolution, satisfactory results were obtained, except for some local morphological features.

In the second application, two field sites, Cocoa Beach and Perdido Key Beach in Florida, were used to explore the capability of the model to simulate offshore mound evolution in deeper water exposed to varying non-breaking waves and water levels. In addition, several scenarios involving different mound volumes and locations were designed to investigate potential uses of the model. The simulation results were in good agreement with the measurements, indicating that the model is sufficiently reliable to simulate the evolution of offshore mounds. Thus, the model can be a useful tool for assisting coastal engineers and managers to design offshore mounds.

In the last application, two laboratory cases from SUPERTANK laboratory data collection project and three field cases from Ocean City, Maryland and Myrtle Beach, South Carolina were employed to investigate dune erosion. The simulations produced good agreement with the measured profile. However, the model did not reproduce post-storm beach recovery.

Overall, the model yields robust and reliable predictions of CS sediment transport and profile evolution, which is promising for practical applications in coastal engineering and management.

## 6 References

- Anthony, E., 2005. Beach erosion. *Encyclopedia of Coastal Science*, Springer, Dordrecht: 140-145.
- Armaroli, C., Grottooli, E., Harley, M.D. and Ciavola, P., 2013. Beach morphodynamics and types of foredune erosion generated by storms along the Emilia-Romagna coastline, Italy. *Geomorphology*, 199: 22-35.
- Bagnold, R., 1940. Beach formation by waves: some model experiments in a wave tank. (includes photographs) *Journal of the Institution of Civil Engineers*, 15(1): 27-52.
- Barnard, P.L., Hanes, D.M., Lescinski, J. and Elias, E., 2007. Monitoring and modeling nearshore dredge disposal for indirect beach nourishment, Ocean Beach, San Francisco. *Proc. Int. Conf. Coastal Engineering 2006*, World Scientific, 5: 4192-4204.
- Bascom, W.N., 1951. The relationship between sand size and beach-face slope. *Eos, Transactions American Geophysical Union*, 32(6): 866-874.
- Bird, E.C., 1996. *Beach management*. Coastal Morphology and Research, 5. John Wiley & Son Limited.
- Birkemeier, W.A. and Forte, M.F., 2019. Field Research Facility: a users guide to the survey lines dataset. *ERDC/CHL SR-19-5*, U.S. Army Engineer Research and Development Center, Coastal and Hydraulics Laboratory.
- Browder, A.E. and Dean, R.G., 2000. Monitoring and comparison to predictive models of the Perdido Key beach nourishment project, Florida, USA. *Coastal Engineering*, 39(2-4): 173-191.
- Camenen, B. and Larson, M., 2005. A bedload sediment transport formula for the nearshore. *Estuarine, Coastal and Shelf Science*, 63(1-2): 249-260.
- Camenen, B. and Larson, M., 2008. A general formula for noncohesive suspended sediment transport. *Journal of Coastal Research*: 615-627.
- Dally, W.R., 1990. Random breaking waves: a closed-form solution for planar beaches. *Coastal Engineering*, 14(3): 233-263.
- Dally, W.R., Dean, R.G. and Dalrymple, R.A., 1985. A model for breaker decay on beaches. *Proc. Int. Conf. Coastal Engineering 1984*, 82-98.

- Dean, R.G., 1988. Recommendations for placement of dredged sand on Perdido Key Gulf Islands National Seashore. *Report UFL/COEL-88/016*, Univ. of Florida, Gainesville, Fl.
- Dissanayake, P., Brown, J. and Karunarathna, H., 2014. Modelling storm-induced beach/dune evolution: Sefton coast, Liverpool Bay, UK. *Marine Geology*, 357: 225-242.
- Dissanayake, P., Brown, J., Wisse, P. and Karunarathna, H., 2015. Effects of storm clustering on beach/dune evolution. *Marine Geology*, 370: 63-75.
- Erikson, L.H., Larson, M. and Hanson, H., 2007. Laboratory investigation of beach scarp and dune recession due to notching and subsequent failure. *Marine Geology*, 245(1-4): 1-19.
- Grant, W.D. and Madsen, O.S., 1982. Movable bed roughness in unsteady oscillatory flow. *Journal of Geophysical Research: Oceans*, 87(C1): 469-481.
- Grasmeijer, B. and Ruessink, B., 2003. Modeling of waves and currents in the nearshore parametric vs. probabilistic approach. *Coastal Engineering*, 49(3): 185-207.
- Hall, J. and Herron, W., 1950. Test of nourishment of the shore by offshore deposition of sand, Long Branch, New Jersey. *BEB-TM-17*, Engineer Research and Development Center, Beach Erosion Board, Washington DC, USA.
- Harley, M.D. and Ciavola, P., 2013. Managing local coastal inundation risk using real-time forecasts and artificial dune placements. *Coastal Engineering*, 77: 77-90.
- Hearin, J., 2014. Historical analysis of beach nourishment and its impact on the morphological modal beach state in the North Reach of Brevard County, Florida. *Journal of Coastal and Marine Research*, 2(3): 37-53.
- Hearin, J.M., 2012. A detailed analysis of beach nourishment and its impact on the surfing wave environment of Brevard County, Florida, Florida Institute of Technology, Melbourne, Florida.
- Isobe, M., 1985. Calculation and application of first-order cnoidal wave theory. *Coastal Engineering*, 9(4): 309-325.
- Iwagaki, Y. and Noda, H., 1962. Laboratory study of scale effects in two-dimensional beach processes. *Coastal Engineering Proceedings*, 1(8): 14.
- Jayaratne, M.P.R., Rahman, M.R. and Shibayama, T., 2014. A cross-shore beach profile evolution model. *Coastal Engineering Journal*, 56(04): 1450020.
- Johnson, B.D., Kobayashi, N. and Gravens, M.B., 2012. Cross-shore numerical model CSHORE for waves, currents, sediment transport and beach profile evolution. *ERDC/CHL TR-12-22*, U.S. Army Engineer Research and Development Center, Vicksburg, Ms.
- Kajima, R., 1983. On-offshore sediment transport experiment by using large scale wave flume. *Central Res. Inst. of Electrical Power Industry (CRIEPI)*.

- King, C. and Williams, W., 1949. The formation and movement of sand bars by wave action. *The Geographical Journal*, 113: 70-85.
- Kobayashi, N., 1987. Analytical solution for dune erosion by storms. *Journal of Waterway, Port, Coastal, and Ocean Engineering*, 113(4): 401-418.
- Kraus, N.C. and Larson, M., 1988. Beach profile change measured in the tank for large waves 1956-1957 and 1962. *Technical Report, CERC-88-6*, U.S. Army Engineer Waterways Experiment Station, Coastal Engineering Research Center, Vicksburg, Ms.
- Kraus, N.C., Larson, M. and Kriebel, D.L., 1991. Evaluation of beach erosion and accretion predictors. *Proc. Int. Conf. Coastal Sediments*, ASCE, 572-587.
- Kraus, N.C. and Smith, J.M., 1994. SUPERTANK laboratory data collection project. *TR-CERC-94-3*, U.S. Army Engineer Waterways Experiment Station, Coastal Engineering Research Center, Vicksburg, Ms.
- Kriebel, D.L., 1995. Swash zone wave characteristics from SUPERTANK. *Proc. Int. Conf. Coastal Engineering 1994*, 2207-2221.
- Kriebel, D.L. and Dean, R.G., 1985. Numerical-simulation of time-dependent beach and dune erosion. *Coastal Engineering*, 9(3): 221-245.
- Kriebel, D.L., Kraus, N.C. and Larson, M., 1991. Engineering methods for predicting beach profile response. *Proc. Int. Conf. Coastal Sediments*, ASCE, 557-571.
- Larson, M., 1995. Model for decay of random waves in surf zone. *Journal of Waterway, Port, Coastal, and Ocean Engineering*, 121(1): 1-12.
- Larson, M., Erikson, L. and Hanson, H., 2004a. An analytical model to predict dune erosion due to wave impact. *Coastal Engineering*, 51(8-9): 675-696.
- Larson, M. and Hanson, H., 2015. Model of the evolution of mounds placed in the nearshore. *Revista de Gestão Costeira Integrada-Journal of Integrated Coastal Zone Management*, 15(1): 21-33.
- Larson, M. and Kraus, N.C., 1989. SBEACH: Numerical model for simulating storm-induced beach change. Report 1. Empirical foundation and model development. *Technical Report CERC-89-9*, U.S. Army Engineer Waterways Experiment Station, Coastal Engineering Research Center, Vicksburg, Ms.
- Larson, M., Kubota, S. and Erikson, L., 2004b. Swash-zone sediment transport and foreshore evolution: field experiments and mathematical modeling. *Marine Geology*, 212(1): 61-79.
- Larson, M., Westergren, S. and Hanson, H., 2015. Modeling beach profile response to varying waves and water levels with special focus on the subaerial region. *Proc. Int. Conf. Coastal Sediments 2015*, World Scientific, San Diego, USA.
- Lindemer, C., Plant, N., Puleo, J.A., Thompson, D. and Wamsley, T., 2010. Numerical simulation of a low-lying barrier island's morphological response to Hurricane Katrina. *Coastal Engineering*, 57(11-12): 985-995.

- Luijendijk, A. et al., 2018. The state of the world's beaches. *Scientific reports*, 8(1): 1-11.
- Madsen, O., 1993. Sediment transport on the shelf. *Sediment Transport Workshop DRP TAI*, U.S. Army Engineer Waterways Experiment Station, Coastal Engineering Research Center, Vicksburg, Ms.
- Madsen, O.S., 1991. Mechanics of cohesionless sediment transport in coastal waters. *Proc. Int. Conf. Coastal sediments*, ASCE, USA, 15-27.
- McCall, R.T. et al., 2010. Two-dimensional time dependent hurricane overwash and erosion modeling at Santa Rosa Island. *Coastal Engineering*, 57(7): 668-683.
- Miller, R.L., 1968. Experimental determination of run-up of undular and fully developed bores. *Journal of Geophysical Research*, 73(14): 4497-4510.
- Nam, P.T., Larson, M. and Hanson, H., 2009. A numerical model of nearshore waves, currents, and sediment transport. *Coastal Engineering*, 56(11): 1084-1096.
- Nielsen, P., 1981. Dynamics and geometry of wave-generated ripples. *Journal of Geophysical Research: Oceans*, 86(C7): 6467-6472.
- Nielsen, P., 1992. *Coastal bottom boundary layers and sediment transport*, 4. World Scientific Publishing Co. Inc.
- Nishi, R. and Kraus, N.C., 1996. Mechanism and calculation of sand dune erosion by storms. *Proc. Int. Conf. Coastal Engineering 1996*, 3034-3047.
- O'Connor, B.A., Pan, S., Nicholson, J., MacDonald, N. and Huntley, D.A., 1998. A 2D model of waves and undertow in the surf zone. *Coastal Engineering Proceedings*, 1(26).
- Otay, E., 1994. *Long term evolution of disposal berms*, University of Florida: Gainesville, FL, USA.
- Overton, M., Fisher, J. and Fenaish, T., 1987. Numerical analysis of swash forces on dunes. *Proc. Int. Conf. Coastal Sediments*, ASCE, 632-641.
- Overton, M., Pratikto, W., Lu, J. and Fisher, J., 1994. Laboratory investigation of dune erosion as a function of sand grain size and dune density. *Coastal Engineering*, 23(1-2): 151-165.
- Owens, E., 1977. Temporal variations in beach and nearshore dynamics. *Journal of Sedimentary Research*, 47(1).
- Palmsten, M.L. and Holman, R.A., 2012. Laboratory investigation of dune erosion using stereo video. *Coastal Engineering*, 60: 123-135.
- Rattanapitikon, W. and Shibayama, T., 2000. Simple model for undertow profile. *Coastal Engineering Journal*, 42(01): 1-30.
- Reniers, A., Roelvink, J. and Walstra, D., 1995. Validation study of UNIBEST-TC; validation against the LIP 11D experiment. *Report H2130*, Delft Hydraulics.

- Rivero, F.J. and S-Arcilla, A., 1993. Propagation of linear gravity waves over slowly varying depth and currents. *Proc. Int. Conf. Ocean Wave Measurement and Analysis*, ASCE, 518-532.
- Roelvink, D. et al., 2009. Modelling storm impacts on beaches, dunes and barrier islands. *Coastal Engineering*, 56(11): 1133-1152.
- Ruessink, B., Kuriyama, Y., Reniers, A., Roelvink, J. and Walstra, D., 2007. Modeling cross-shore sandbar behavior on the timescale of weeks. *Journal of Geophysical Research: Earth Surface*, 112(F3).
- Sallenger Jr, A.H., 2000. Storm impact scale for barrier islands. *Journal of Coastal Research*: 890-895.
- Sloss, C., 2012. Coastal dunes: geomorphology. *Nature Education Knowledge*, 3(3): 1-7.
- Smith, E.R., D'Alessandro, F., Tomasicchio, G.R. and Gailani, J.Z., 2017a. Nearshore placement of a sand dredged mound. *Coastal Engineering*, 126: 1-10.
- Smith, E.R., Mohr, M.C. and Chader, S.A., 2017b. Laboratory experiments on beach change due to nearshore mound placement. *Coastal Engineering*, 121: 119-128.
- Smith, E.R., Permenter, R., Mohr, M.C. and Chader, S.A., 2015. Modeling of nearshore-placed dredged material. *Report ERDC/CHL TR-15-9*, U.S. Army Engineer Research and Development Center, Vicksburg, Ms.
- Soulsby, R., 1997. *Dynamics of marine sands: a manual for practical applications*. Thomas Telford.
- Southgate, H.N. and Nairn, R.B., 1993. Deterministic profile modelling of nearshore processes. Part 1. Waves and currents. *Coastal Engineering*, 19(1-2): 27-56.
- Steetzel, H.J., 1990. Cross-shore transport during storm surges. *Coastal Engineering Proceedings*, 1(22).
- Swart, D.H., 1974. Offshore sediment transport and equilibrium beach profiles, TU Delft, Delft University of Technology. <http://resolver.tudelft.nl/uuid:057cb136-5f5b-484a-878d-5616fbaeda4e>.
- United Nations, 2017. Factsheet: people and oceans. *The Ocean Conference 2017*, New York, 1-7.
- USACE, 1984. *Shore protection manual*. US Government Printing Office, Washington, DC.
- Van Rijn, L. and Walstra, D., 2004. Analysis and modelling of shoreface nourishments. *Report WL/Delft Hydraulics Z3748*.

- Van Rijn, L. et al., 2003. The predictability of cross-shore bed evolution of sandy beaches at the time scale of storms and seasons using process-based profile models. *Coastal Engineering*, 47(3): 295-327.
- Van Rijn, L. and Wijnberg, K., 1996. One-dimensional modelling of individual waves and wave-induced longshore currents in the surf zone. *Coastal Engineering*, 28(1-4): 121-145.
- van Rijn, L.C., 1984. Sediment transport, part III: bed forms and alluvial roughness. *Journal of Hydraulic Engineering*, 110(12): 1733-1754.
- van Rijn, L.C., 2009. Prediction of dune erosion due to storms. *Coastal Engineering*, 56(4): 441-457.
- Vousdoukas, M.I. et al., 2020. Sandy coastlines under threat of erosion. *Nature Climate Change*, 10(3): 260-263.
- Watts, G.M. and Dearduff, R.F., 1954. Laboratory study of effect of tidal action on wave-formed beach profiles, Beach Erosion Board Technical Memorandum No. 52. Department of the Army. <http://hdl.handle.net/11681/3432>.
- Williams, J., Brown, J., Esteves, L. and Souza, A., 2011. MICORE WP4 Modelling coastal erosion and flooding along the Sefton Coast NW UK, final report.
- Wilson, K., 1989. Friction of wave-induced sheet flow. *Coastal Engineering*, 12(4): 371-379.
- Wise, R.A., Smith, S. and Larson, M., 1996. SBEACH: Numerical model for simulating storm-induced beach change. Report 4. Cross-shore transport under random waves and model validation with SUPERTANK and field data. *Technical Report CERC-89-9*, U.S. Army Engineer Waterways Experiment Station, Coastal Engineering Research Center, Vicksburg, Ms.
- Work, P., 1990. *Perdido Key Beach Nourishment Project: Gulf Islands National Seashore (Pre-nourishment Survey-Conducted October 28-November 3, 1989)*. Coastal and Oceanographic Engineering Department, University of Florida.
- Work, P.A. and Otay, E.N., 1997. Influence of nearshore berm on beach nourishment. *Proc. Int. Conf. Coastal Engineering 1996*, 3722-3735.
- Wright, L., Nielsen, P., Shi, N. and List, J., 1986. Morphodynamics of a bar-trough surf zone. *Marine Geology*, 70(3-4): 251-285.
- Xu, J. and Wright, L., 1995. Tests of bed roughness models using field data from the Middle Atlantic Bight. *Continental Shelf Research*, 15(11-12): 1409-1434.





**LUND**  
UNIVERSITY

Lund University  
Faculty of Engineering  
Department of Building and Environmental Technology  
Water Resources Engineering

ISBN 978-91-7895-875-7

ISSN 1101-9824

CODEN: LUTVDG/TVVR-1090 (2021)

